OAK RIDGE NATIONAL LABORATORY
MANAGED BY UT-BATTELLE FOR THE DEPARTMENT OF ENERGY

ORNL-GEN4/LTR-06-019

Experimental Plan and Final Design Report for HFIR High Temperature Graphite Irradiation Capsules HTV-1 and -2

T. Burchell, D. Heatherly, J. McDuffee, D. Sparks, and K. Thoms

GEN IV Nuclear Energy Systems

August 31, 2006

UT-BATTELLE
OAK RIDGE NATIONAL LABORATORY

This report was prepared as an account of work sponsored by an agency of the United States Government. Neither the United States government nor any agency thereof, nor any of their employees, makes any warranty, express or implied, or assumes any legal liability or responsibility for the accuracy, completeness, or usefulness of any information, apparatus, product, or process disclosed, or represents that its use would not infringe privately owned rights. Reference herein to any specific commercial product, process, or service by trade name, trademark, manufacturer, or otherwise, does not necessarily constitute or imply its endorsement, recommendation, or favoring by the United States Government or any agency thereof. The views and opinions of authors expressed herein do not necessarily state or reflect those of the United States Government or any agency thereof.

Experimental Plan and Final Design Report for HFIR High Temperature Graphite Irradiation Capsules HTV-1 and -2

T. Burchell, D. Heatherly, J. McDuffee, D. Sparks, and K. Thoms
Oak Ridge National Laboratory

August 31, 2006

Prepared for
Office of Nuclear Energy Science and Technology

Prepared by
OAK RIDGE NATIONAL LABORATORY
Oak Ridge, Tennessee 37831
managed by
UT-BATTELLE, LLC
for the
U.S. DEPARTMENT OF ENERGY
Under DOE Contract No. DE-AC05-00OR22725

This page intentionally left blank

TABLE OF CONTENTS

Page

List of Figures iv

List of Tables v

Acronyms vi

Executive Summary vii

1. Objectives 1

2. Introduction 1

3. Background 4
   3.1 Displacement Damage 4
   3.2 Mechanism of Dimensional Change Behavior 4

4. Materials and Test Conditions 8
   4.1 Materials 8
   4.2 Test Conditions 9
   4.3 Irradiation Specimen Geometries 10

5. HTV Capsule Design and Layout 10
   5.1 Capsule Design 10
   5.2 Thermal Analysis 14
      5.2.1 Heat Generation Rates 14
      5.2.2 Finite Element Thermal Analysis 16
   5.3 Loading Scheme 23

6. Materials Pre-characterization 28

7. Post-irradiation Examination 31

8. Schedule 33

9. Acknowledgements 33

10. References 33

List of Figures

Page

Figure 2.1. HTV capsule conceptual design drawing 3

Figure 3.1. Displacement damage mechanism in graphite 4

Figure 3.2. Neutron irradiation damage mechanism in graphite showing the induced crystal dimensional changes 5

Figure 3.3. Irradiation-induced volume changes for H-451 graphite at two irradiation temperatures [6] 6

Figure 3.4. Dimensional change behavior of H-451 graphite at an irradiation temperature of 600°C [6] 7

Figure 3.5. Dimensional change behavior of H-451 graphite at an irradiation temperature of 900°C [6] 7

Figure 5.1. Subcapsule assembly 11

Figure 5.2. Melt-material container design 12

Figure 5.3. Centering thimble design 12

Figure 5.4. Grafoil separator design 13

Figure 5.5. Subcapsule 1 design with grafoil spacers 13

Figure 5.6. Target Region of HFIR Showing the HTV Capsule in Positions B1-C1-C2 14

Figure 5.7. MCNP Model of the HTV Capsules 15

Figure 5.8. MCNP Axial Heat Generation Profiles for BOC, EOC, and Design 16

Figure 5.9. ANSYS model for (1) the grafoil spacer with dosimetry inserts and (2) the sacrificial "specimen" containing melt-materials for post-irradiation temperature analysis. 17

Figure 5.10. Comparison of a an actual centering thimble with the axisymmetric model 18

Figure 5.11. Subcapsule ANSYS model 18

Figure 5.12. Specimen Temperatures for HTV-1 19

Figure 5.13. Specimen Temperatures for HTV-2 20

Figure 5.14. Temperature profile for subcapsule 1 in HTV-1. This subcapsule has the largest temperature variation of all subcapsules. Temperature is in ºK. 21

Figure 5.15. Estimated dose (dpa) and temperature distributions for capsules HTV-1 and -2 28

Figure 6.1. Preirradiation data process flow chart for irradiation experiments HTV-1 and -2 30

Figure 7.1. The postirradiation examination process for HFIR experiments HTV-1 and-2 32

List of Tables

Page

Table 4.1. Experiment HTV-1 and -2 graphite materials test matrix 8

Table 4.2. Capsule HTV-1 and -2 graphite grades, vendors, and available processing information.....8

Table 4.3. The number of samples and their graphite grades included in irradiation capsules HTV-1 and -2 9

Table 4.4. Property data for the grades in Capsules HTV-1 and -2 to be used in capsule design 9

Table 4.5. Capsule HTV-1 and -2 anticipated peak neutron damage doses 10

Table 5.1. Material heat generation rates for BOC, EOC, and design.....17

Table 5.2. Melt-material temperature summary (ºC) 21

Table 5.3. Maximum spacer temperature summary (ºC) 22

Table 5.4. Summary of the holder outside diameters 22

Table 5.5. Neutron dose per sample in each capsule and temperature zone for grade H-451 (reference graphite).....23

Table 5.6. Neutron dose per sample in each capsule and temperature zone for grade PCEA 23

Table 5.7. Neutron dose per sample in each capsule and temperature zone for grade NBG-17.....24

Table 5.8. Neutron dose per sample in each capsule and temperature zone for grade NBG-18.....25

Table 5.9. Neutron dose per sample in each capsule and temperature zone for grade IG-430.....26

Table 6.1. Graphite grade marking codes to be used for the HTV series of experiments 29

Table 8.1. Planned schedule for Capsules HTV-1 and -2.....33

Acronyms

AG	against-grain
AGC	ATR-Graphite-Creep
ASME	American Society of Mechanical Engineers
ASTM	American Society for Testing and Materials
ATR	Advanced Test Reactor
BOC	Beginning of cycle
EOC	End of cycle
GTHTR	Gas Turbine High Temperature Reactor
HFIR	High Flux Isotope Reactor
HMP	horizontal mid-plane of HFIR
HTGR	high temperature gas-cooled reactor
HTV	HFIR-Target-VHTR
ID	inside diameter
INL	Idaho National Laboratory
JAERI	Japan Atomic Energy Research Institute
NBG	Nuclear Block Graphite
NGNP	Next Generation Nuclear Plant
NNFD	Non-reactor Nuclear Facilities Division
OD	outside diameter
ORNL	Oak Ridge National Laboratory
PBMR	Pebble Bed Modular Reactor
PIE	post irradiation examination
SEM	scanning electron microscope
SiC	silicon carbide
VHTR	very high temperature reactor
WG	with-grain

Executive Summary

Here we report the objectives, technical plan, schedule, and final design details for the High Flux Isotope Reactor (HFIR) target irradiation experiments HTV-1 and -2. Experiments HTV-1 and -2 will be irradiated in the HFIR target region to a peak irradiation dose of ~2.2 x 10^{21} n/cm^2 [E > 0.1 MeV] or ~1.6 displacements per atom (dpa) and ~6.5 x 10^{21} n/cm^2 [E > 0.1 MeV] or ~4.8 dpa, respectively. Each capsule has multiple temperature zones allowing irradiation temperatures of 900, 1200, and 1500°C.

The key data to be obtained from these capsules include:

- Elastic constants (Young's modulus, E; Shear modulus, G; Poisson's ratio, ?)
- Dimensional Change
- Thermal conductivity, room temperature, and elevated temperature
- Compressive strength
- Microstructural characterization

These data are critical to the design of the NGNP and the high-temperature graphite irradiation creep capsule (AGC) planned for irradiation in the Advanced Test Reactor (ATR) at Idaho National Laboratory (INL). Moreover, the data supports ongoing work in the area of model development; e.g., irradiation effect models such as dimensional change, structural modeling, and fracture modeling. Moreover, the data will be used to underpin the American Society of Mechanical Engineers (ASME) design code currently being prepared for graphite core components.

The report reviews the background and theory of irradiation-induced dimensional change in graphites, and details the graphite grades to be irradiated in the experiment along with the rationale for their inclusion. Details of the irradiation test conditions are reported. Detailed capsule layout plans are reported for HTV-1 and -2, and the specimens are tabulated by grade, location, and anticipated fluence. Details of the capsule design, including the capsule thermal analysis are discussed. The process of pre- and post-irradiation examination is reported and details of the tests to be performed and the data to be acquired are given. Finally, the schedule for HTV-1 and -2 is reported.

1. Objectives

The primary objective of irradiation capsules HTV-1 and -2 is to provide high-temperature irradiation dimensional change data to support the design of the high-temperature (1200°C) AGC creep experiment being planned for the ATR at INL, and design data to support the development of the next generation nuclear plant (NGNP). Specifically, data for the effects of neutron irradiation on the dimensional stability, strength, elastic modulus, and thermal conductivity of candidate NGNP graphites will be obtained in the temperature range 900-1500°C.

2. Introduction

HTV-1 and -2 are High Flux Isotope Reactor (HFIR) high-temperature irradiation capsules designed to provide dimensional change and physical property data for the NGNP program, and to support the design of ATR high-temperature creep experiments (AGC series of capsules) [1]. The HTV-1 and -2 capsules will reach peak doses of ~1.59 and ~4.76 displacements per atom (dpa), respectively, and each capsule contains temperature zones designed to operate at either 900, 1200, or 1500°C. The data to be obtained from these irradiation capsules includes:

- Irradiation induced volume and dimensional changes
- Irradiation induced density changes
- The effect of irradiation on the room temperature and elevated temperature thermal conductivity
- The effect of irradiation on the elastic constants, Young's modulus, E; Shear modulus, G; Poisson's ratio, ?.
- The effect of irradiation on the compressive strength.

The graphite grades to be included in the HTV capsules are: SGL grade NBG-18, which is the candidate-grade for pebble bed modular reactor (PBMR) core structures; NBG-17, which is a finer-grained version of NBG-18 and is a candidate for the prismatic block reactor fuel elements and core structures; GrafTech grade PCEA which is a candidate for the prismatic block reactor fuel elements and core structures; Toyo Tanso grade IG-430 which is Japan Atomic Energy Research Institute's (JAERI) preference for their Gas Turbine High Temperature Reactor (GTHTR) 300 concept; SGL grade H-451 will be included as a reference grade to link with historical data. Further details of the materials are given in Section 4.

The graphite specimens for the HTV-1 and -2 capsules are solid cylinders with a nominal 5.3-mm thickness and an outer diameter of 10.2 mm, 8.9 mm, or 7.6 mm, depending on the target specimen temperature and location. There are a total of eight subcapsules in each capsule, and eight specimens in each subcapsule, for a total of 64 specimens per capsule and 128 total specimens. Each subcapsule will have a design temperature of 900°C, 1200°C, or 1500°C.

The temperature in each subcapsule is controlled by setting the gas gap between the subcapsule outside diameter (OD) and the aluminum housing inside diameter (ID). The capsules will be

sealed and filled with neon gas. Details of the capsule loading plans are given in Section 5. A schematic drawing of the HTV capsule design is given in Figure 2.1.

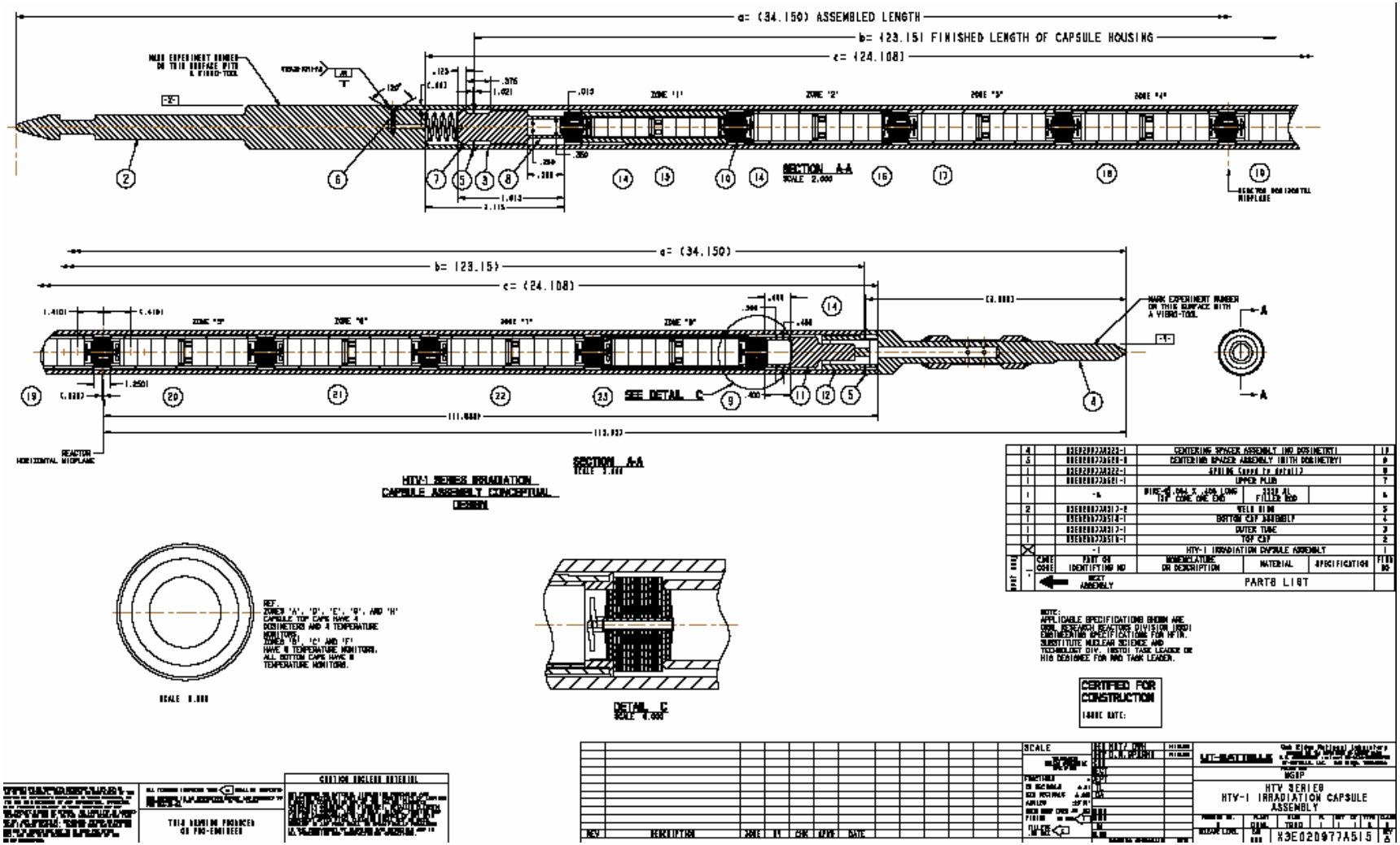

Figure 2.1. HTV capsule conceptual design drawing

3. Background

3.1 Displacement Damage

Radiation damage in graphite occurs when energetic particles, such as fast neutrons, impinge on the crystal lattice and displace carbon atoms from their equilibrium positions–creating a lattice vacancy and an interstitial carbon atom. The displaced carbon atoms recoil through the lattice and produce other carbon atom displacements in a cascade effect. The cascade carbon atoms tend to be clustered in small groups of 5-10 atoms, and it is generally satisfactory to treat the displacements as if they occur randomly. However, not all of the carbon atoms remain displaced. The displaced carbon atoms diffuse between the graphite layer planes in two dimensions and a high proportion of them will recombine with lattice vacancies. Others will coalesce to form linear molecules, which in turn may form the nucleus of a dislocation loop — essentially a new graphite plane. Interstitial clusters, on further irradiation, may be destroyed by impinging neutrons or energetic displaced carbon atoms (irradiation annealing). Adjacent lattice vacancies in the same graphite crystal basal plane are believed to collapse parallel to the basal plane, thereby forming sinks for other vacancies that are increasingly mobile above 600EC, and hence, can no longer recombine and annihilate interstitials. This mechanism is illustrated in Figure 3.1. The lattice strain that results from displacement damage causes significant structural and property changes in the graphite.

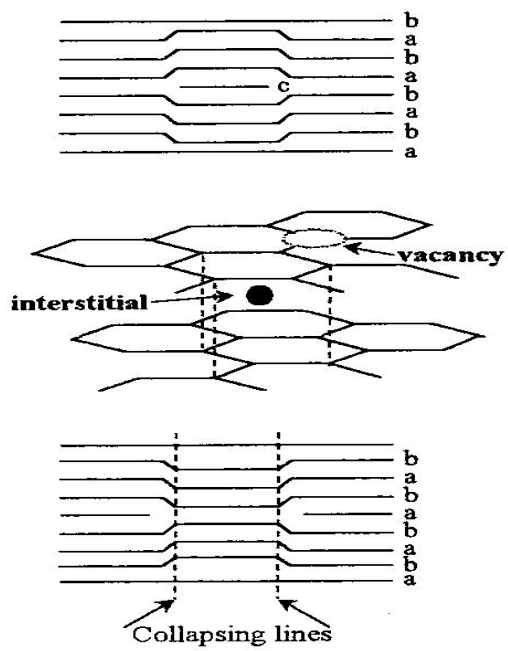

Figure 3.1. Displacement damage mechanism in graphite

3.2 Mechanism of Dimensional Change Behavior

A principal result of the carbon atom displacements discussed above is crystalline dimensional change. Interstitial defects will cause crystallite growth perpendicular to the layer planes (c-axis

direction), whereas coalescence of vacancies will cause a shrinkage parallel to the layer planes (a-axis direction). The damage mechanism and associated dimensional changes are illustrated in Figure 3.2.

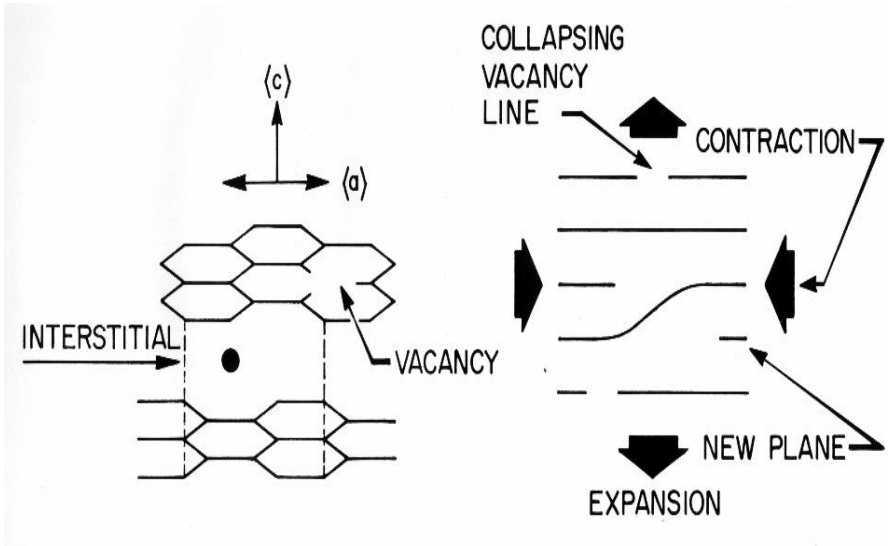

Figure 3.2. Neutron irradiation damage mechanism in graphite showing the induced crystal dimensional changes

Polygranular graphite exhibits a polycrystalline structure, usually with significant texture resulting from the method of forming during manufacture. Consequently, structural and dimensional changes in polygranular graphite are a function of the crystallites dimensional change and the graphite's texture. In polygranular graphite, thermal shrinkage cracks (formed during manufacture) that are preferentially aligned in the crystallographic a-direction initially accommodate the c-direction expansion, so mainly a-direction contraction is observed. Hence, the graphite undergoes net volume shrinkage. This behavior is illustrated with data from grade H-451 graphite, an extruded grade used in the Fort St. Vrain HTGR. As seen in Figure 3.3, H-451 exhibits volume shrinkage behavior at irradiation temperatures of 600 and 900°C. With increasing neutron dose (displacements), the incompatibility of crystallite dimensional changes leads to the generation of new porosity, and the volume shrinkage rate falls, eventually reaching zero. The graphite then begins to swell at an increasing rate with increasing neutron dose because of the combined effect of c-axis growth and new pore generation. The graphite thus undergoes a volume change "turnaround" into net growth which continues until the generation of cracks and pores in the graphite, due to differential crystal strain, eventually causes total disintegration of the graphite (Figure 3.3).

At low irradiation temperatures, typically < 300°C, volume growth may be observed initially, followed by the rapid onset of volume shrinkage [2, 3]. The low dose volume swelling has been attributed to the relaxation of fabrication stresses [3, 4]. With increasing dose the volume shrinkage behavior would be expected to turnaround to net swelling [5].

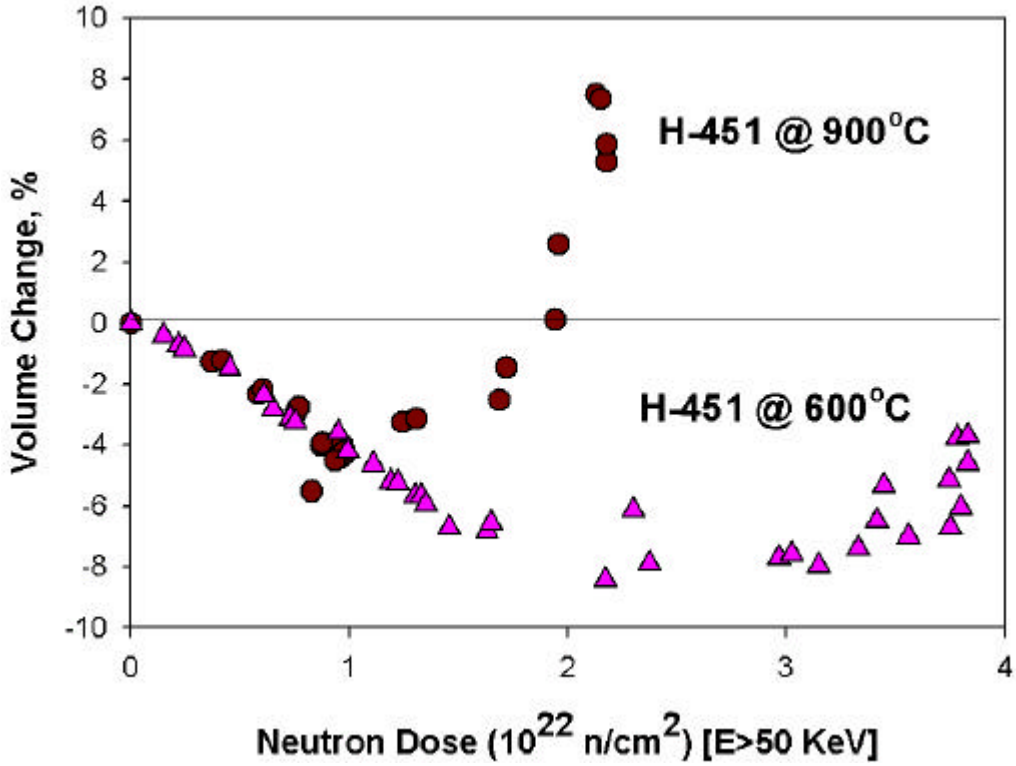

Figure 3.3. Irradiation-induced volume changes for H-451 graphite at two irradiation temperatures [6]

H-451 graphite is an extruded material and thus the filler coke particles are preferentially aligned in the extrusion axis (parallel direction). Consequently, the crystallographic a-direction is preferentially aligned in the parallel direction and the a-direction shrinkage is more apparent in the parallel (to extrusion) direction, as indicated by the parallel direction dimensional change data in Figure 3.4 and Figure 3.5. The dimensional and volume changes are greater at an irradiation temperature of 600°C than at 900°C, i.e., both the maximum shrinkage and the turnaround dose are greater at an irradiation temperature of 600°C. This temperature effect can be attributed to the thermal closure of internal porosity aligned parallel to the a-direction that accommodates the c-direction swelling. At higher irradiation temperatures a greater fraction of this accommodating porosity is closed, and thus the shrinkage is less at the point of turnaround. While considerable data exists for the behavior of graphites at temperatures in the range 300-900°C much less is available for temperatures > 900°C. Hence there is a clear need for the HTV-1 and -2 experiments.

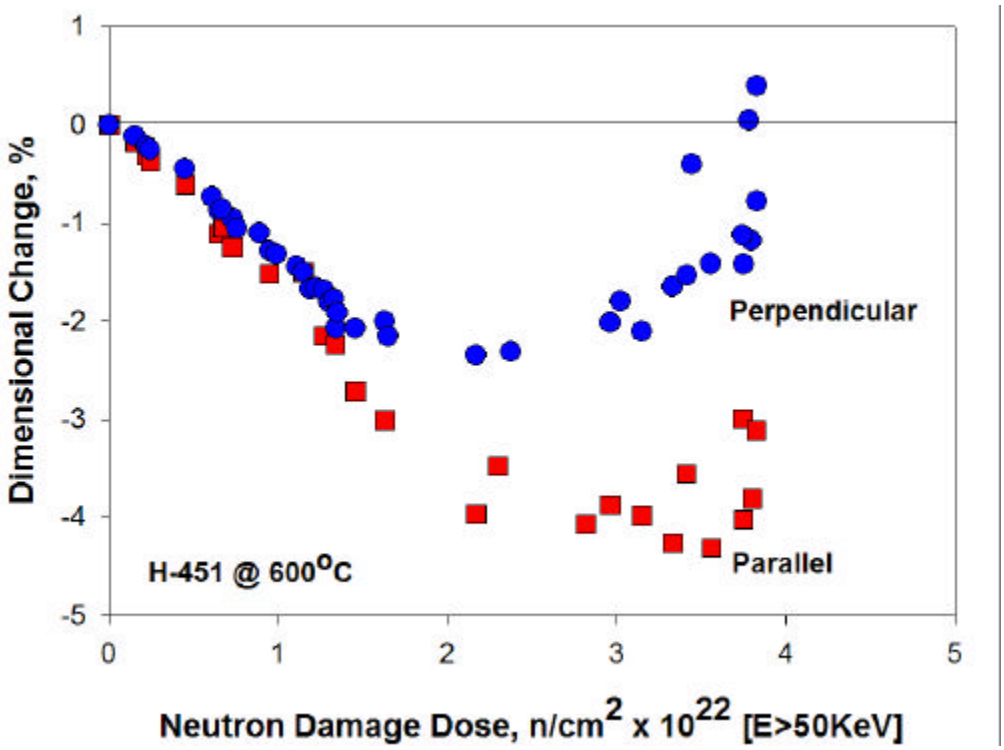

Figure 3.4. Dimensional change behavior of H-451 graphite at an irradiation temperature of 600°C [6]

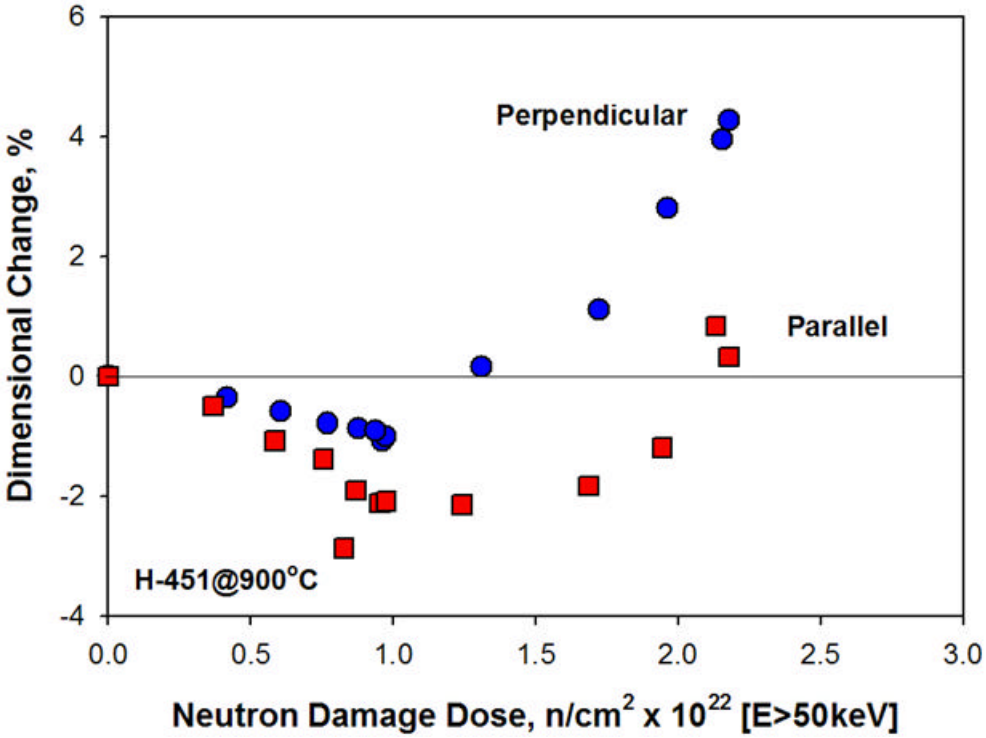

Figure 3.5. Dimensional change behavior of H-451 graphite at an irradiation temperature of 900°C [6]

4. Materials and Test Conditions

4.1 Materials

The graphites to be included in HTV-1 and -2 are given in Table 4.1 along with information on their potential application to the NGNP program. The grades to be included are PCEA, NBG-17, NBG-18, IG-430, and the reference grade H-451. Graphite grades, vendors, and available processing information are given in Table 4.2.

Table 4.1. Experiment HTV-1 and -2 graphite materials test matrix

Graphite	Reactor Vendor	Proposed Use	Capsule Location	Remarks
H-451	General Atomics	Prismatic fuel element and replaceable reflector	900°C zones only	Historical Reference Only a few samples
PCEA	AREVA	Prismatic fuel and replaceable block	All temp. zones	AREVA wants to construct the entire graphite core out of the same graphite
NBG-18	PBMR	Pebble bed reflector structure and insulation blocks	All temp. zones	Candidate for PBMR replaceable reflector and core structures
NBG-17	AREVA	Prismatic Fuel element and replaceable reflector	All temp. zones	AREVA wants to construct the entire graphite core out of the same graphite. NBG-17 is finer grain than NBG-18
IG-430	JAERI	Prismatic fuel element, replaceable reflector, and core support pedestals	All temp. zones	JAERI wants to use this graphite in the GTHTR 300

Table 4.2. Capsule HTV-1 and -2 graphite grades, vendors, and available processing information

Graphite Grade	Source	Country of Origin	Process Details
NBG-17	SGL Carbon	Germany/France	Pitch coke, vibrationally molded, medium grain
NBG-18	SGL Carbon	Germany/France	Pitch coke, vibrationally molded, medium grain
H-451 (Reference Grade)	SGL Carbon	USA	Petroleum coke, extruded, medium grain No longer in production
PCEA	GrafTech International	USA	Petroleum coke, extruded, medium grain
IG-430	Toyo Tanso	Japan	Pitch coke, isostatically molded, fine grain

Table 4.3 reports the number of specimens per grade in capsules HTV-1 and -2. Details of the locations of these specimens within each capsule are given in Section 5.

Table 4.3. The number of samples and their graphite grades included in irradiation capsules HTV-1 and -2

Graphite Grade	Source	Number of Samples per capsule	
		HTV-1	HTV-2
NBG-17	SGL Carbon	16	16
NBG-18	SGL Carbon	16	16
PCEA	GrafTech International	16	16
IG-430	Toyo Tanso	14	13
H-451 (Reference Grade)	SGL Carbon	2	3
	TOTAL	64	64

The key physical properties of the graphites in capsules HTV-1 and -2 are given in Table 4.4. These data are also used in the thermal design of the capsule. Note that POCO Graphite grade AXF-5Q is used as a barrier between the specimens and the niobium subcapsules.

Table 4.4. Property data for the grades in Capsules HTV-1 and -2 to be used in capsule design

Grades	Density g/cm^3	Coefficient of thermal expansion 10^{-6}/ºC	Unirradiated thermal conductivity (nominal) W/m-ºK	Unirradiated thermal conductivity [Figure5B.03 except POCO] [7]			Irradiated thermal conductivity ($\Phi > 2\cdot10^{21}$ n/cm^2 E > 0.18 MeV) W/m-ºK
				900ºC W/m-ºK	1200ºC W/m-ºK	1500ºC W/m-ºK	
PCEA	1.83	5.1 / 5.6* (T > 1000ºC)	165 (WG)	74.9	62.2	54.6	43.8
IG430	1.82	4.8 (350<T<450ºC)	139	63.1	52.4	46.0	36.9
NBG-17	1.88	4.5/4.6* (20 < T < 200ºC)	150	68.1	56.6	49.7	39.9
NBG-18	1.85	4.5/4.5*	150	68.1	56.6	49.7	39.9
POCO AXF-5Q	1.80	8.4	~95	43.1	35.8	31.4	29.6

***WG/AG**

4.2 Test Conditions

Capsules HTV-1 and -2 are HFIR target rod design capsules. The HTV-1 and -2 capsules will reach peak doses of ~1.59 and ~4.76 dpa, respectively, and each capsule contains temperature zones designed to operate at either 900, 1200, or 1500°C. Each capsule contains eight subcapsules, and each subcapsule contains eight specimens, for a total of 64 specimens per capsule and 128 total specimens. Each subcapsule is designed for a specific temperature, which is controlled by setting the gas gap between the subcapsule OD and the aluminum housing ID. The capsules will be filled with neon gas and sealed. A schematic drawing of the HTV capsule design is given in Figure 2.1. Appendix A contains a detailed breakdown of the temperature and fluence design for HTV-1 and -2.

The HTV experiments will contain a series of flux wires, and the post-irradiation data from these wires will be used to calibrate the flux models and yield improved dose estimates for each

specimen in the capsule. In addition, the center specimen position of each subcapsule will contain melt-material temperature monitors to help establish the actual irradiation temperature of each subcapsule.

Capsule HTV-1 is a one-cycle experiment, while HTV-2 will remain in the HFIR core for three cycles. The HFIR flux spectrum is symmetrical about the reactor mid-plane, and thus, by careful arrangement of the samples, a useful range of doses may be attained for each graphite grade. The anticipated peak dose in capsules HTV-1 and -2 are reported in Table 4.5 in dose units of dpa and n/cm^2. The detailed specimen loading configuration is discussed in Section 5.3.

Table 4.5. Capsule HTV-1 and -2 anticipated peak neutron damage doses

Capsule	Peak Damage Dose		
	dpa	**n/cm^2 [E>0.1 MeV]***	**n/cm^2 [E>50 keV]$^{\#}$**
HTV-1	1.59	0.22×10^{22}	0.23×10^{22}
HTV-2	4.76	0.65×10^{22}	0.70×10^{22}

***** To convert n/cm^2 [E>0.1 MeV] to dpa multiply by 7.3×10^{-22}
$^{\#}$ To convert n/cm^2 [E>50 keV] to dpa multiply by 6.8×10^{-22}

4.3 Irradiation Specimen Geometries

The graphite specimens for the HTV-1 and -2 capsules are solid cylinders with a nominal 5.3-mm thickness and an outer diameter of 10.2 mm, 8.9 mm, or 7.6 mm, depending on the target specimen temperature and location. Billet cutting plans will be developed for each of the graphites to be included in the HTV capsules. The cutting plans will take into account spatial variations and anisotropy considerations resulting from graphite forming (textural effects). Additionally, the cutting plans will identify a specimen numbering scheme that will assure a unique identity for each specimen traceable to the grade, billet numbers, and position within the graphite billet. The billet cutting plans will be reported in the HTV-1 and -2 preirradiation data report. Specimens will be cut with their thickness direction parallel to the forming axis [WG for extrusion (PCEA) and AG for molding (NBG-17 and -18)]. Grade IG-430 is isotropic, but the specimen thickness direction will be oriented parallel to the major axis of the billet.

5. HTV Capsule Design and Layout

5.1 Capsule Design

The HTV capsules are divided into eight subcapsules, each with eight specimens. The basic capsule layout is shown in Figure 2.1. Each subcapsule is comprised of five concentric cylinders, as shown in Figure 5.1. The innermost cylinder is a stack of eight specimens and one graphite melt-material container, which is fabricated to the same shape and size as a specimen. The specimens in the stack will all have the same outer diameter of 10.2 mm, 8.9 mm, or 7.6 mm, depending on the temperature and location of the subcapsule. The melt-material container, shown in Figure 5.2, is always at the axial center position.

The specimen stack is surrounded by a 0.5-mm thick POCO graphite sleeve, which prevents contact between the specimens and the third layer – the niobium holder. Sandwiched between the niobium holder and the outer aluminum housing is a thin layer of neon gas.

The temperature in the subcapsule is controlled by the thickness of the neon gas layer between the niobium holder and aluminum housing. The holder has different ODs at the top, middle, and bottom to compensate for heat losses through the subcapsule ends and for the heating profile, which peaks at the horizontal mid-plane (HMP) of the reactor and falls off toward the top and bottom.

A centering thimble, shown in Figure 5.3, is inserted into the top and bottom of each holder. This part holds the specimens in position inside the holder and centers the subcapsule inside the housing. The prongs of the thimble are designed to hold the subcapsule in place while minimizing the heat losses through the subcapsule ends. Small wires are inserted through matching holes in the holder and thimble to ensure the thimbles stay in place during assembly and irradiation.

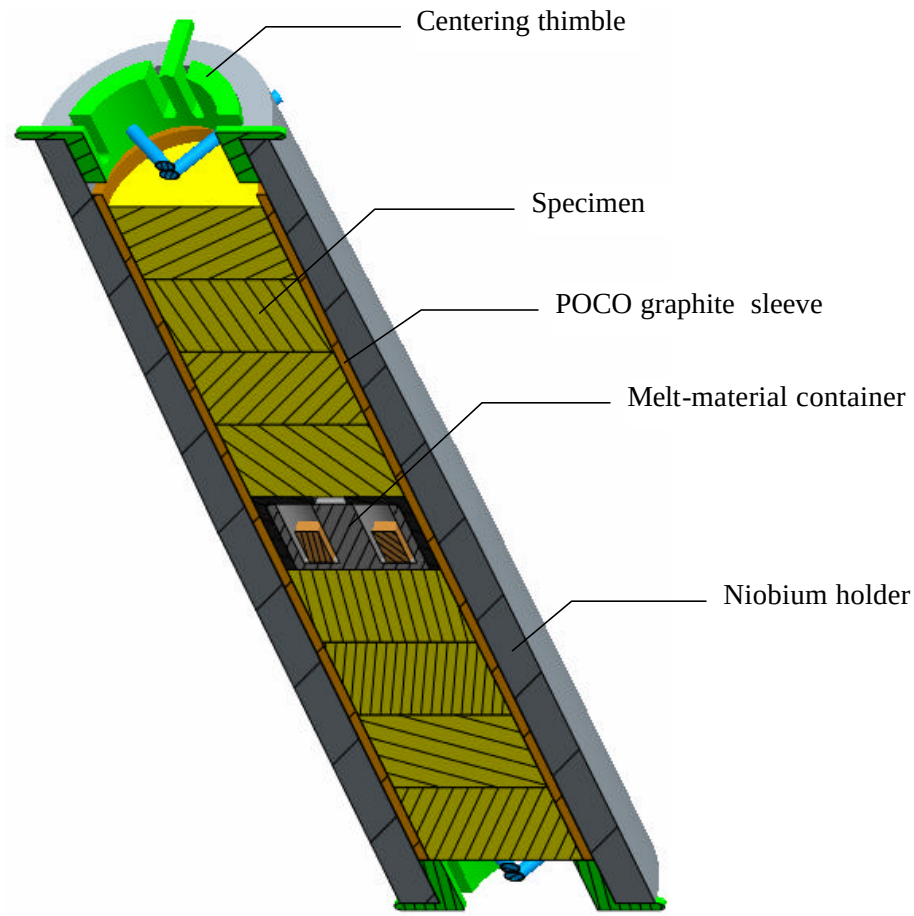

Figure 5.1. Subcapsule assembly

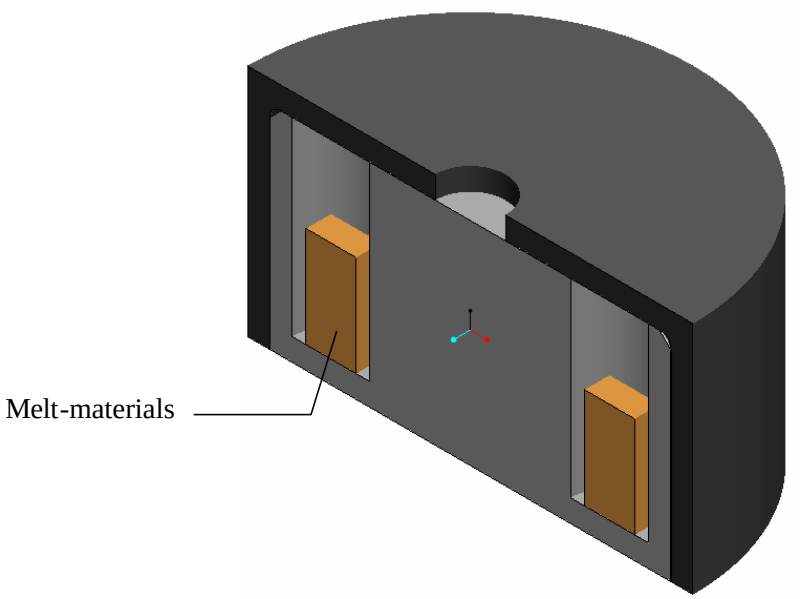

Figure 5.2. Melt-material container design

Figure 5.3. Centering thimble design

The subcapsules are separated with stacked sheets of thin grafoil wafers splined on a thin-walled molybdenum tube, as shown in Figure 5.4. Each end of a stack is fitted with a shoulder that is sized to insert inside the inner diameter of a centering thimble. Dosimetry parts are inserted into the grafoil assembly. Figure 5.5 shows a view of the top subcapsule with the grafoil spacer inserts.

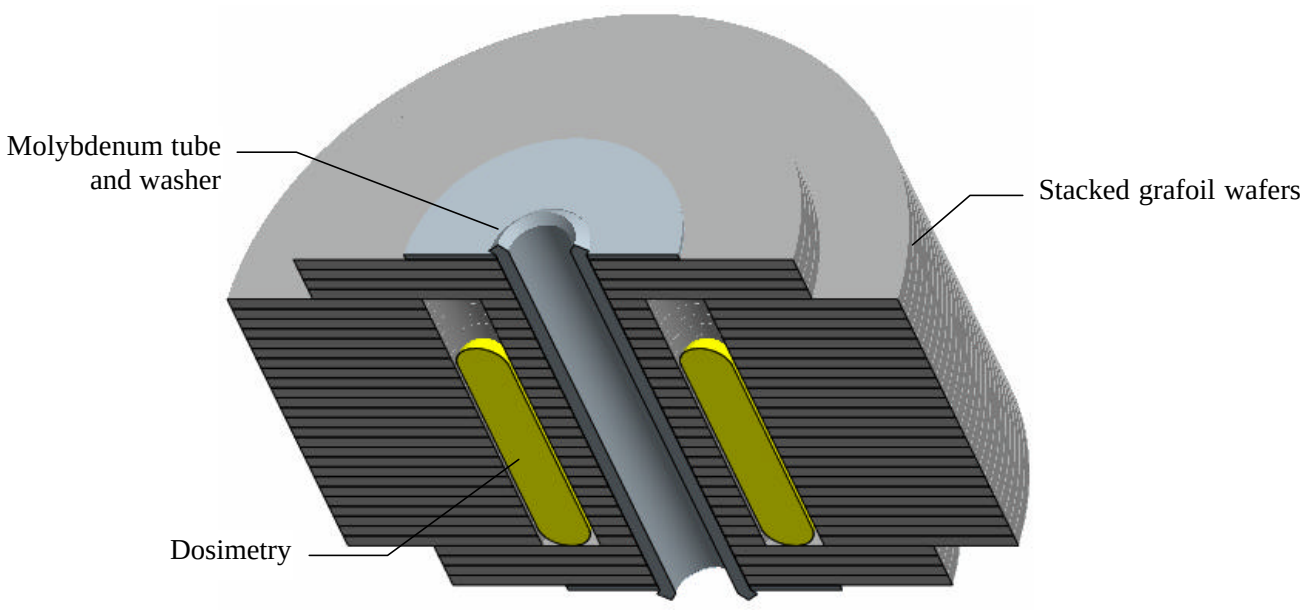

Figure 5.4. Grafoil separator design

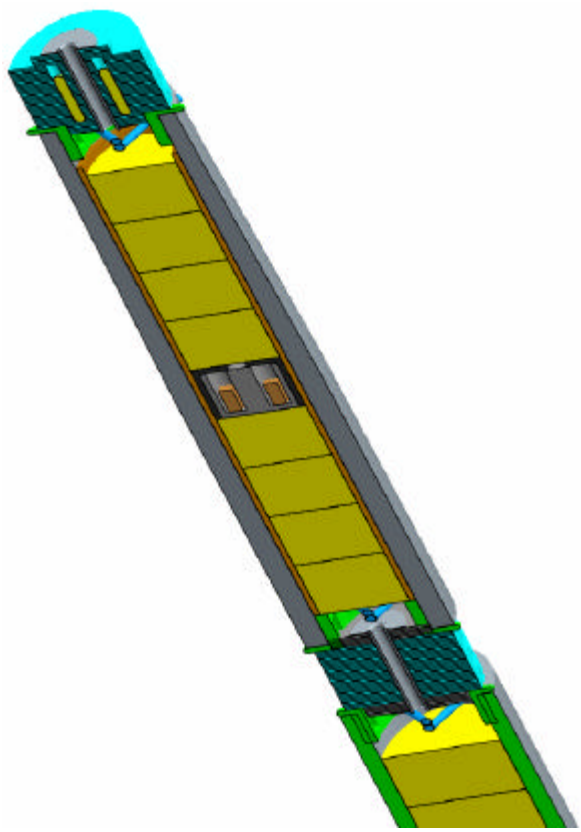

Figure 5.5. Subcapsule 1 design with grafoil spacers

5.2 Thermal Analysis

The thermal analysis and design of the HTV capsules is accomplished in two steps: (1) determination of appropriate heat generation rates and (2) a coupled thermal/structural analysis that includes the conduction, convection, and radiation solution and the thermal expansion of the capsule parts. MCNP Version 5 [8] is the primary tool used to estimate heat generation rates. The ANSYS [9] finite element model is used to solve the coupled thermal/structural solution.

5.2.1 Heat Generation Rates

The MCNP model used to estimate the heat generation rates of the HTV materials is shown in Figure 5.6 and Figure 5.7. The loading configuration is based on the actual HFIR loading for Cycle 400. The trefoil shroud is simplified into a simple cylinder with the same coolant flow area and cross sectional area. This will preserve the water and aluminum volume in the capsule, which is important for accurately estimating neutron moderating affects. The gap size is not important for this calculation, so a constant holder diameter of 0.5" (12.7 mm) is assumed for all holders. The model was developed with both beginning-of-cycle (BOC) and end-of-cycle (EOC) fuel loading/control plate configuration options.

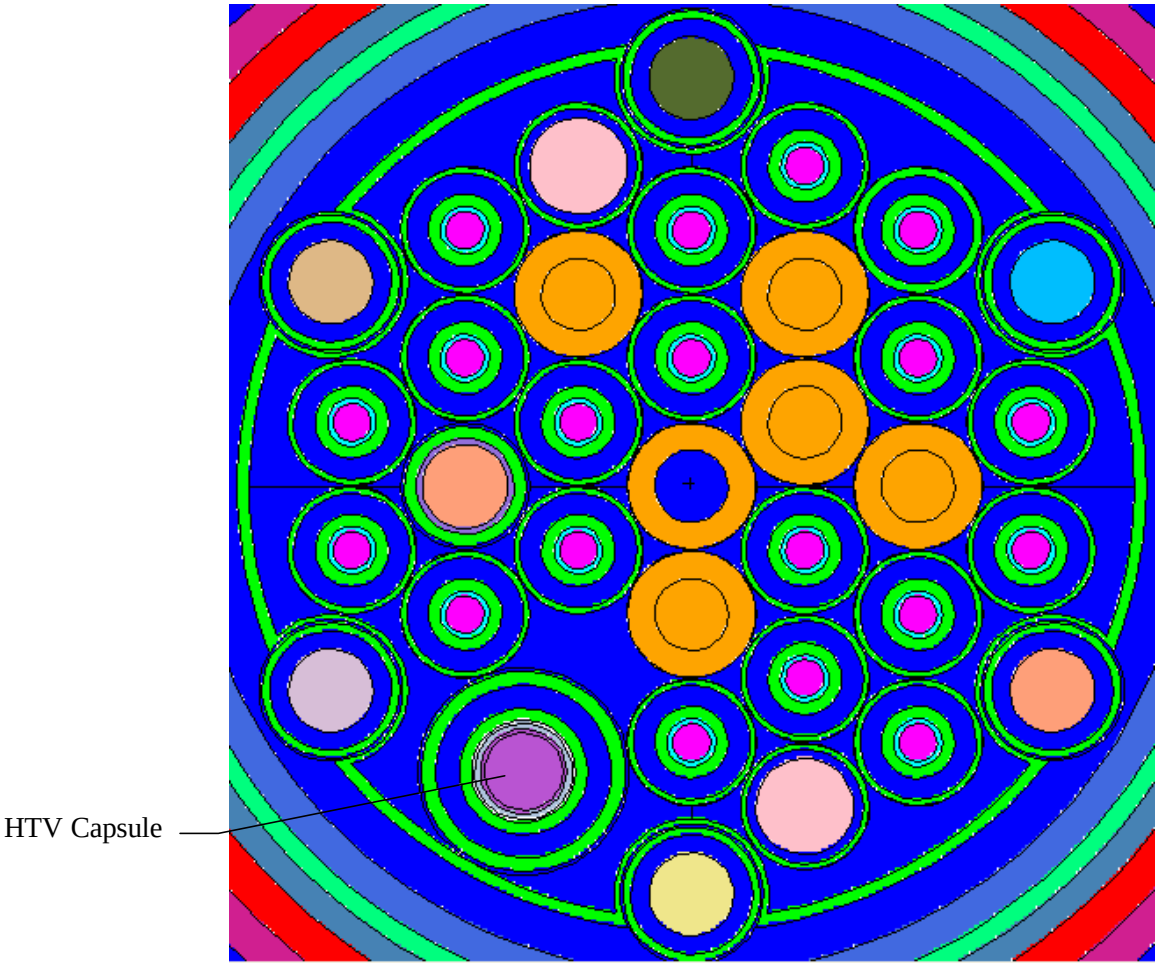

Figure 5.6. Target Region of HFIR Showing the HTV Capsule in Positions B1-C1-C2

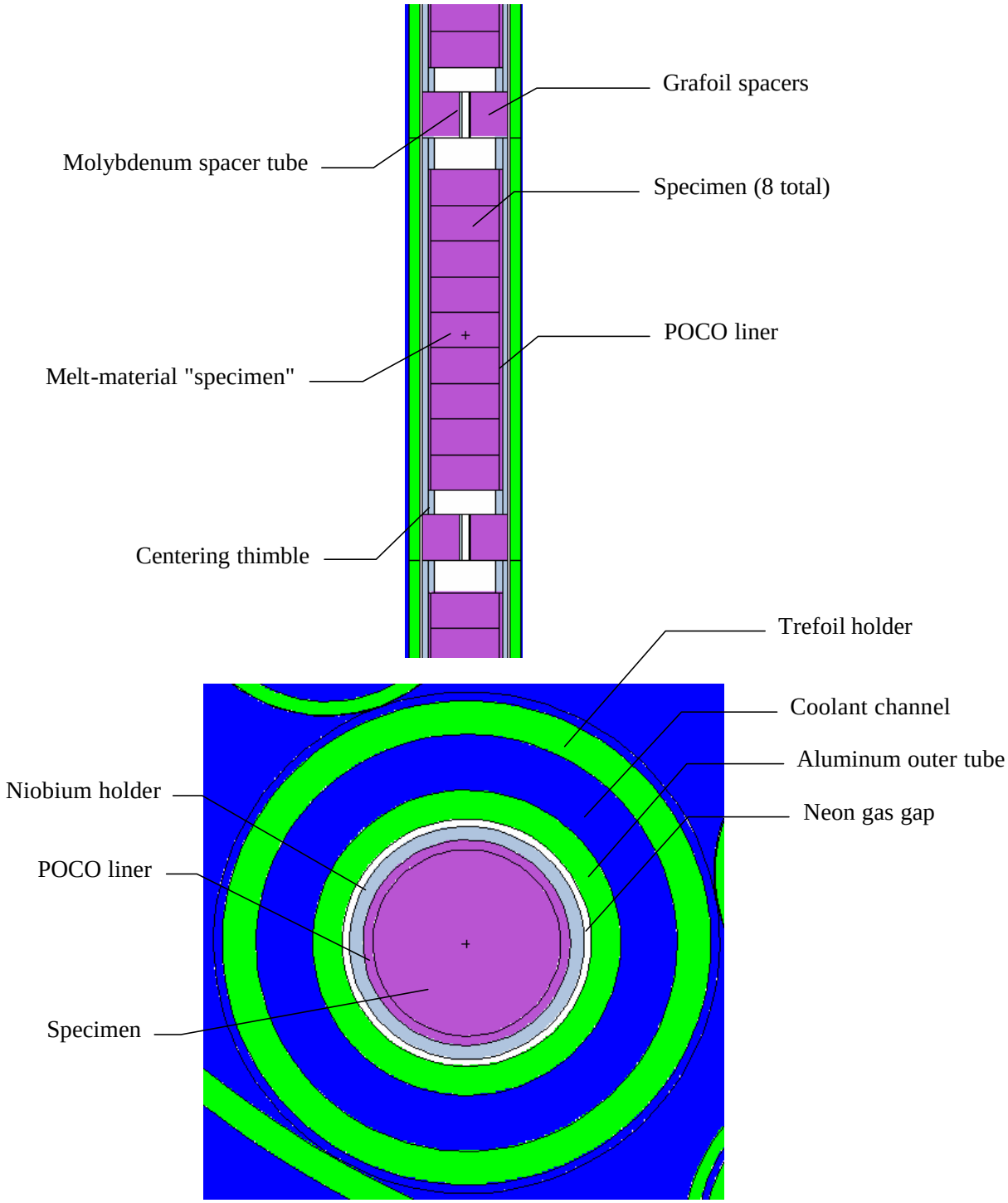

Figure 5.7. MCNP Model of the HTV Capsules

The MCNP model was run in (n,p) mode using a fission source (kcode) to obtain the neutron energy absorption rate (e.g., due to neutron scattering and [n,?] reactions) and the direct photon absorption rate from direct fission photons. A second calculation was developed to obtain the energy absorption due to photons originating from fission product decay. In this calculation, photons are assumed to originate in the core with the same radial and axial distribution as

fissions in the original kcode calculation. The energy distribution of the fission product photons and the number of photons per fission was estimated using ORIGEN-S [10].

Figure 5.8 shows the heat generation axial profile for both BOC and EOC based on the MCNP results for the graphite specimens. A composite curve fit was developed as a design basis. There is about a 10% change in the peak heat generation rate from BOC to EOC. However, the heat generation rate towards the top and bottom remains relatively constant. Table 5.1 summarizes the peak heat generation rates for BOC, EOC, and design.

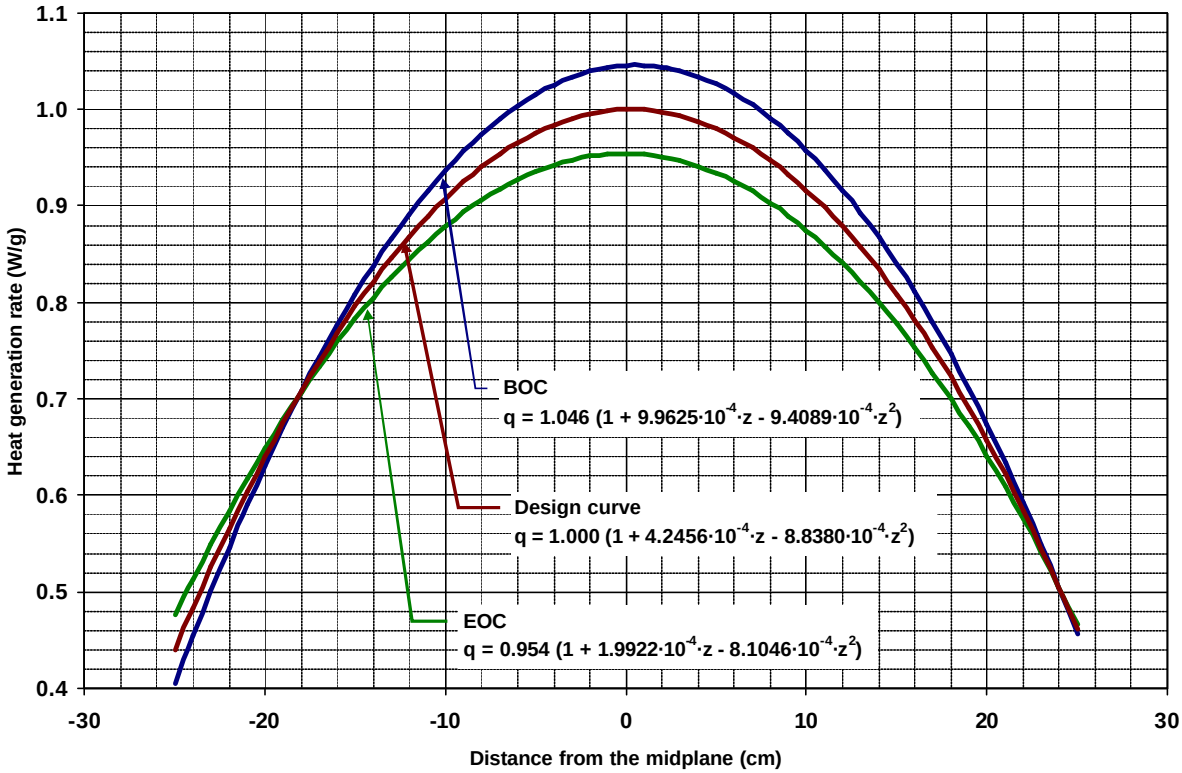

Figure 5.8. MCNP Axial Heat Generation Profiles for BOC, EOC, and Design

5.2.2 Finite Element Thermal Analysis

The HTV-1 and -2 capsules are modeled in the ANSYS finite element program with an axisymmetric model that spans the full length of the outer trefoil shroud. There are three parts within the capsules that have non-axisymmetric features: (1) the melt-material "specimens", (2) the dosimetry inserts in the grafoil separators, and (3) the centering thimbles. Both the melt-materials and the dosimetry inserts are very small parts that do not significantly affect the surrounding temperature profile. These items are modeled very approximately as vanadium-filled holes, as shown in Figure 5.9.

Table 5.1. Material heat generation rates for BOC, EOC, and design

Material	Decay	BOC			EOC			Total Design
		Prompt Fission	Fission Product Decay	Total	Prompt Fission	Fission Product Decay	Total	
Graphite	---	21.8	12.6	34.4	20.6	10.7	31.3	32.8
Grafoil	---	22.5	12.8	35.3	20.1	11.6	31.7	33.5
Niobium	---	32.6	26.4	59.0	30.0	24.0	54.0	56.5
Molybdenum	0.3	33.5	27.2	61.0	28.8	27.9	57.0	59.0
Vanadium	19.4	22.2	11.4	53.0			53.0*	53.0
Al 6061	1.5	20.1	13.4	35.0	18.1	11.9	31.5	33.0

**Vanadium is a minor component that does not significantly affect the temperature profile. An EOC calculation was not done for this material.*

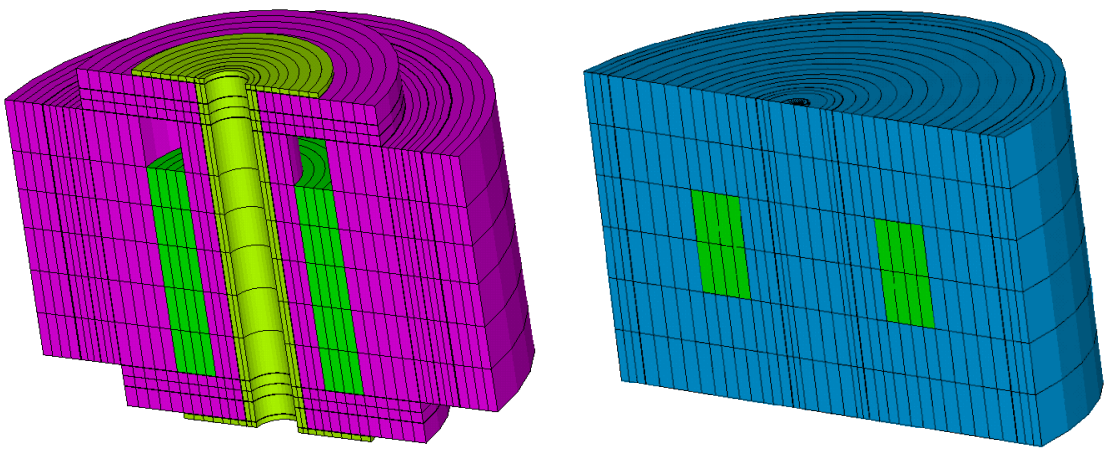

Figure 5.9. ANSYS model for (1) the grafoil spacer with dosimetry inserts and (2) the sacrificial "specimen" containing melt-materials for post-irradiation temperature analysis.

In contrast, the centering thimbles are key components that control the amount of heat loss through the ends of each subcapsule. An axisymmetric approximation was developed by maintaining the total contact surface area, as shown in Figure 5.10.

All the remaining parts are fundamentally axisymmetric, and no significant geometrical changes are required for the model. However, some features of the end parts at the top and bottom of the capsules are neglected because they are not relevant to the temperature profile inside the subcapsules. Figure 5.11 shows the total axisymmetric model of a representative subcapsule. Note that all solid parts are separated by a 0.5 mil (0.0127 mm) neon gas layer to simulate the effects of thermal contact resistance.

Drawing of an actual centering thimble *Axisymmetric model of a centering thimble*

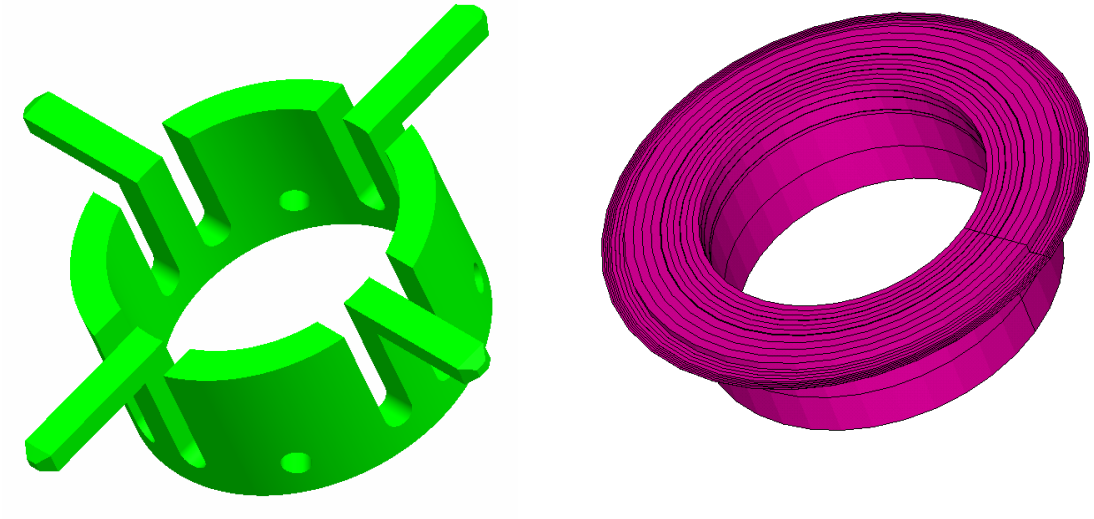

Figure 5.10. Comparison of an actual centering thimble with the axisymmetric model

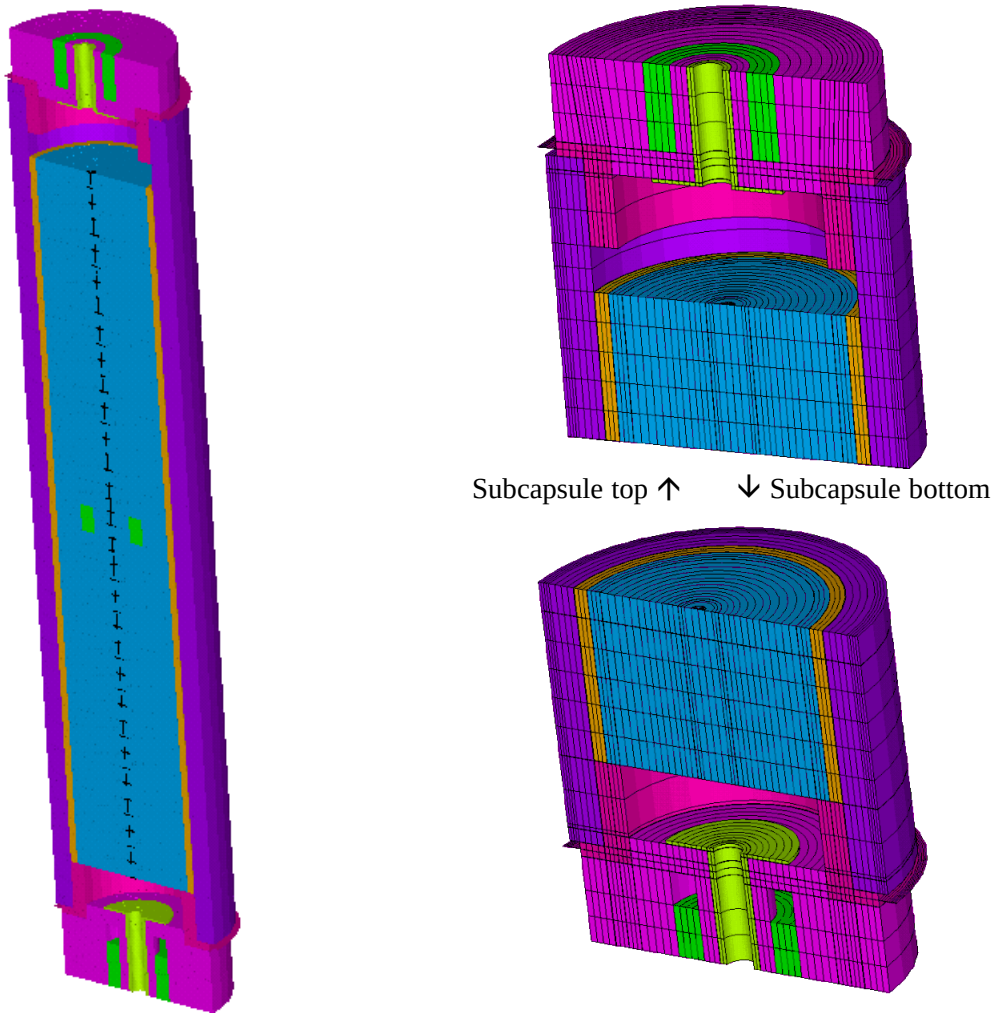

Figure 5.11. Subcapsule ANSYS model

As described in Section 5.1, the temperature goal for each subcapsule is achieved by selecting outer holder diameters at the top, middle, and bottom of each subcapsule. The specimen temperatures for HTV-1 and HTV-2 are shown in Figure 5.12 and Figure 5.13, respectively. The specimen types are shown by color. The minimum and maximum specimen temperatures are shown as error bars. (Note that the error bars do not represent uncertainty, but rather the as-modeled temperature range for each specimen.) Figure 5.14 shows the temperature contour for subcapsule 1 of HTV-1, which has the largest specimen temperature variation of all subcapsules.

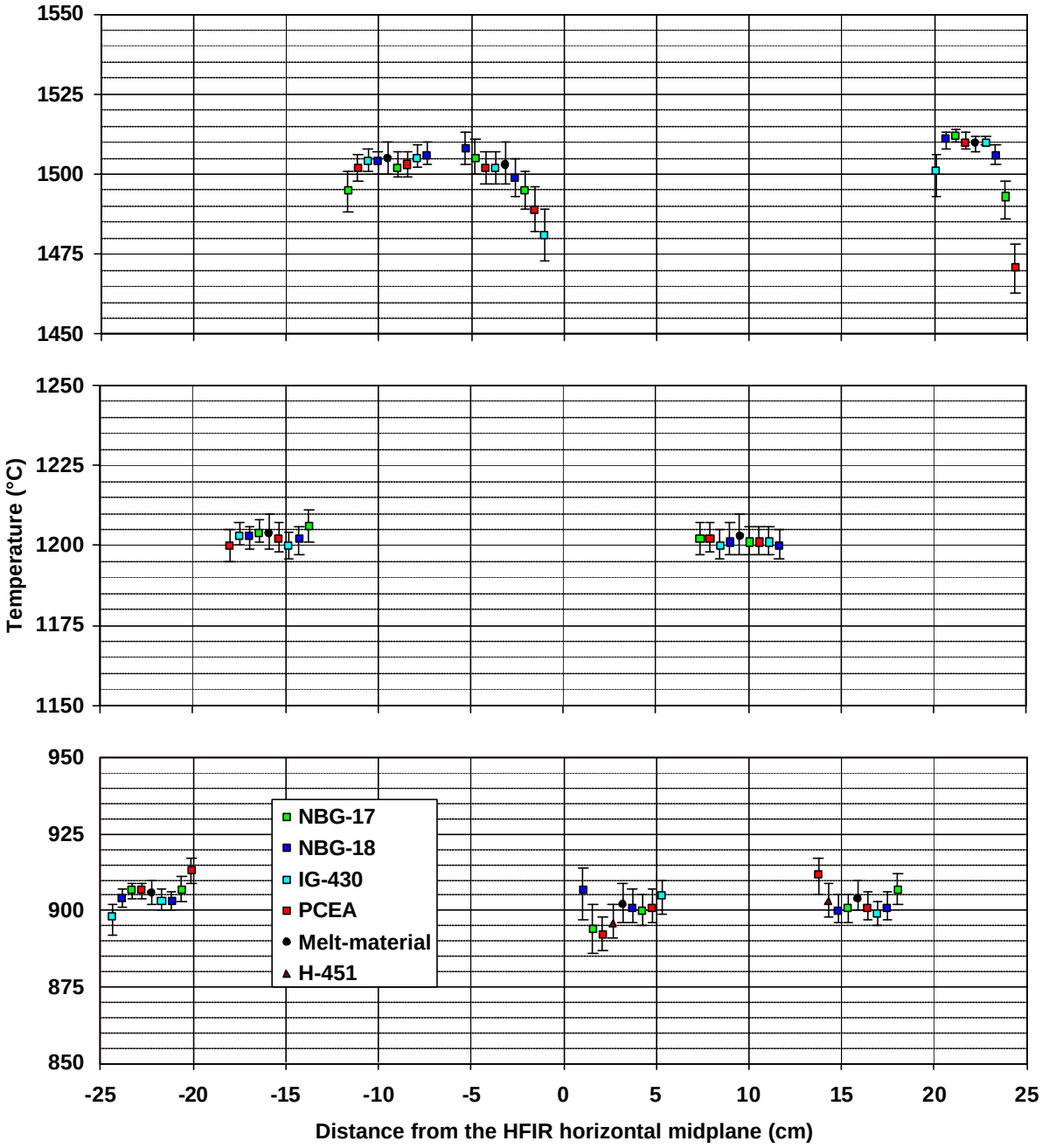

Figure 5.12. Specimen Temperatures for HTV-1

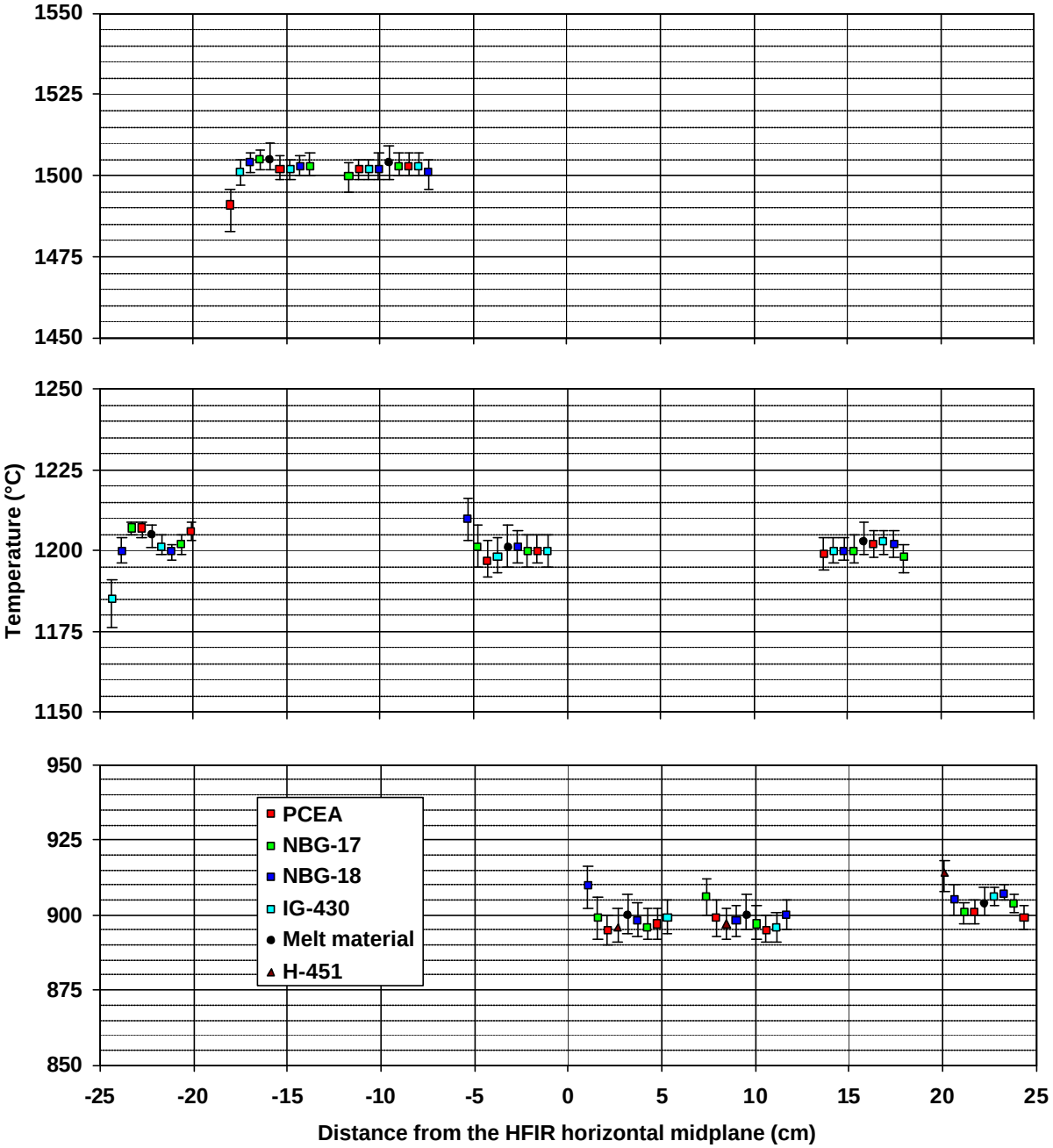

Figure 5.13. Specimen Temperatures for HTV-2

Table 5.2 and Table 5.3 summarize the temperatures for the melt-material specimens and the grafoil spacers, respectively. This information can be used to choose melt-materials and dosimetry materials that are appropriate for the capsule temperatures.

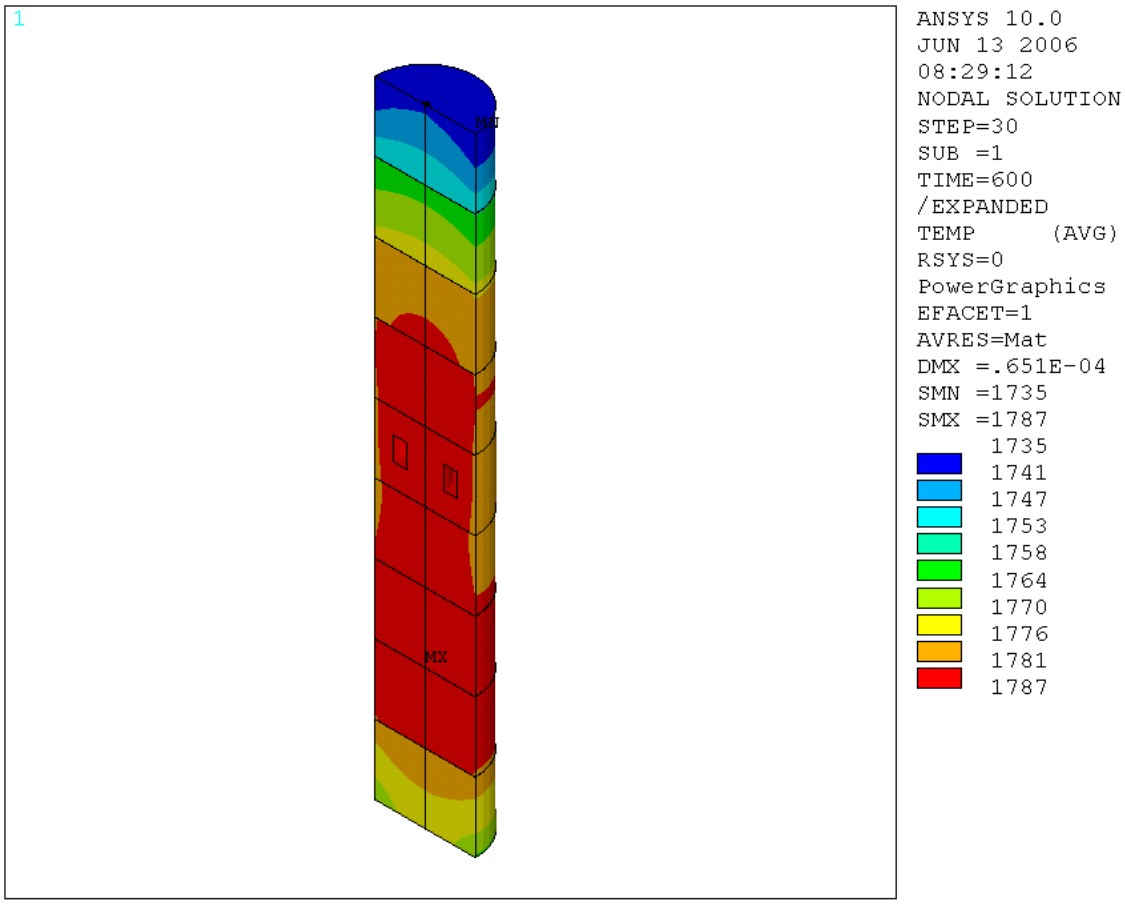

Figure 5.14. Temperature profile for subcapsule 1 in HTV-1. This subcapsule has the largest temperature variation of all subcapsules. Temperature is in ºK.

Table 5.2. Melt-material temperature summary (ºC)

HTV-1	T_{avg}	T_{min}	T_{max}		HTV-2	T_{avg}	T_{min}	T_{max}
1	1510	1508	1513		**1**	904	900	909
2	904	899	910		**2**	1203	1198	1209
3	1203	1197	1210		**3**	900	895	907
4	902	896	910		**4**	900	894	907
5	1503	1497	1510		**5**	1201	1195	1209
6	1505	1500	1510		**6**	1504	1500	1510
7	1204	1200	1210		**7**	1505	1501	1509
8	906	902	910		**8**	1205	1201	1208

Table 5.3. Maximum spacer temperature summary (ºC)

	HTV-1	HTV-2
Top	1361	839
1-2	1466	937
2-3	984	1155
3-4	942	1182
4-5	1174	953
5-6	1188	919
6-7	962	926
7-8	973	947
Bottom	1422	1180

To achieve as much temperature uniformity as possible, the outside diameter of the niobium holders have linear profiles from the top and bottom to the holder axial center. Table 5.4 summarizes the outer diameters for each holder.

Table 5.4. Summary of the holder outside diameters

Subcapsule	Location	HTV-1 (in)	HTV-1 (mm)	HTV-2 (in)	HTV-2 (mm)
1	Top	0.4050	10.29	0.4920	12.50
	Middle	0.5006	12.72	0.5092	12.93
	Bottom	0.4868	12.36	0.5151	13.08
2	Top	0.5162	13.11	0.4884	12.41
	Middle	0.5149	13.08	0.5030	12.78
	Bottom	0.5190	13.18	0.5042	12.81
3	Top	0.5042	12.81	0.5186	13.17
	Middle	0.5082	12.91	0.5178	13.15
	Bottom	0.5088	12.92	0.5198	13.20
4	Top	0.5199	13.21	0.5195	13.20
	Middle	0.5185	13.17	0.5188	13.18
	Bottom	0.5214	13.24	0.5206	13.22
5	Top	0.4735	12.03	0.5097	12.95
	Middle	0.4884	12.41	0.5096	12.94
	Bottom	0.4868	12.36	0.5117	13.00
6	Top	0.5048	12.82	0.5036	12.79
	Middle	0.5051	12.83	0.5049	12.82
	Bottom	0.4992	12.68	0.5014	12.74
7	Top	0.5072	12.88	0.4990	12.67
	Middle	0.5015	12.74	0.4993	12.68
	Bottom	0.4929	12.52	0.4823	12.25

Table 5.4. Summary of the holder outside diameters

Subcapsule	Location	HTV-1 (in)	HTV-1 (mm)	HTV-2 (in)	HTV-2 (mm)
8	Top	0.5140	13.06	0.5080	12.90
	Middle	0.5088	12.92	0.5041	12.80
	Bottom	0.4936	12.54	0.4733	12.02

5.3 Loading Scheme

Details of the HTV capsule loading scheme are given in Appendix 1. As described in Section 5.1, there are eight subcapsules with eight specimens in each subcapsule, resulting in a total of 64 specimens in each capsule. The subcapsules are numbered 1 through 8 from top to bottom. The specimen position numbers consist of two numbers with the first number being the subcapsule number and the second being the cumulative specimen number from the top of the capsule. Thus, capsule position 1-1 is at the top of the experiment and position 8-64 at the bottom. Positions 4-32 and 5-33 are directly above and below the reactor horizontal mid-plane (HMP), respectively. The estimated flux ratio is the result of neutron dosimetry data from past experiments operated in the HFIR target region. The thermal zones of the experiment are color coded as follows, blue-900°C, green-1200°C, and orange-1500°C. Each specimen number and diameter is given along with doses for capsule HTV-1 (one cycle) and capsule HTV-2 (three cycles). The specimens are numbered sequentially from capsule top to bottom, specimens D1 through F14 in capsule HTV-1 and specimens D17 through F27 in capsule HTV-2.

The following series of tables reports the neutron dose per specimen in each temperature zone for each of the grades included in capsules HTV-1 and -2. The rows within each table are in order of increasing dose (within each capsule) so one may easily see the spread of doses attained at each experimental irradiation temperature. This information is also shown graphically in Figure 5.15.

Table 5.5. Neutron dose per sample in each capsule and temperature zone for grade H-451 (reference graphite)

Capsule	Position	Specimen Number	Grade	Dose, dpa	Temperature, C
HTV-1	2-15	C1	H-451	1.29	900
HTV-1	4-29	C2	H-451	1.58	900
HTV-2	1-8	C3	H-451	2.97	900
HTV-2	3-22	C4	H-451	4.45	900
HTV-2	4-29	C5	H-451	4.73	900

Table 5.6. Neutron dose per sample in each capsule and temperature zone for grade PCEA

Capsule	Position	Specimen Number	Grade	Dose, dpa	Temperature, C
HTV-1	8-61	D16	PCEA	0.82	900
HTV-1	8-57	D15	PCEA	0.99	900

Table 5.6. Neutron dose per sample in each capsule and temperature zone for grade PCEA

HTV-1	2-12	D3	PCEA	1.19	900
HTV-1	2-16	D4	PCEA	1.31	900
HTV-1	4-26	D7	PCEA	1.55	900
HTV-1	4-30	D8	PCEA	1.58	900
HTV-2	1-1	D17	PCEA	2.12	900
HTV-2	1-5	D18	PCEA	2.67	900
HTV-2	3-19	D21	PCEA	4.26	900
HTV-2	3-23	D22	PCEA	4.48	900
HTV-2	4-26	D23	PCEA	4.66	900
HTV-2	4-30	D24	PCEA	4.74	900
HTV-1	7-56	D14	PCEA	1.11	1200
HTV-1	7-52	D13	PCEA	1.24	1200
HTV-1	3-19	D5	PCEA	1.42	1200
HTV-1	3-23	D6	PCEA	1.49	1200
HTV-2	8-61	D32	PCEA	2.46	1200
HTV-2	8-57	D31	PCEA	2.97	1200
HTV-2	2-12	D19	PCEA	3.56	1200
HTV-2	2-16	D20	PCEA	3.92	1200
HTV-2	5-38	D26	PCEA	4.68	1200
HTV-2	5-34	D25	PCEA	4.75	1200
HTV-1	1-1	D1	PCEA	1.44	1500
HTV-1	1-5	D2	PCEA	1.51	1500
HTV-1	6-47	D12	PCEA	1.40	1500
HTV-1	6-43	D11	PCEA	1.48	1500
HTV-1	5-38	D10	PCEA	1.56	1500
HTV-1	5-34	D9	PCEA	1.58	1500
HTV-2	7-56	D30	PCEA	3.32	1500
HTV-2	7-52	D29	PCEA	3.72	1500
HTV-2	6-47	D28	PCEA	4.21	1500
HTV-2	6-43	D27	PCEA	4.45	1500

Table 5.7. Neutron dose per sample in each capsule and temperature zone for grade NBG-17

Capsule	Position	Specimen Number	Grade	Dose, dpa	Temperature, C
HTV-1	2	A1	NBG-17	0.75	900
HTV-1	6	A2	NBG-17	0.92	900
HTV-1	10	A3	NBG-17	1.14	900
HTV-1	14	A4	NBG-17	1.26	900

Table 5.7. Neutron dose per sample in each capsule and temperature zone for grade NBG-17

HTV-1	18	A5	NBG-17	1.4	900
HTV-1	22	A6	NBG-17	1.48	900
HTV-2	2	A17	NBG-17	2.24	900
HTV-2	6	A18	NBG-17	2.87	900
HTV-2	10	A19	NBG-17	3.41	900
HTV-2	14	A20	NBG-17	3.77	900
HTV-1	62	A16	NBG-17	0.79	1200
HTV-1	58	A15	NBG-17	0.96	1200
HTV-1	54	A14	NBG-17	1.17	1200
HTV-1	50	A13	NBG-17	1.28	1200
HTV-1	26	A7	NBG-17	1.55	1200
HTV-1	30	A8	NBG-17	1.58	1200
HTV-2	62	A32	NBG-17	2.37	1200
HTV-2	58	A31	NBG-17	2.87	1200
HTV-2	18	A21	NBG-17	4.21	1200
HTV-2	22	A22	NBG-17	4.44	1200
HTV-2	26	A23	NBG-17	4.66	1200
HTV-2	30	A24	NBG-17	4.74	1200
HTV-1	46	A12	NBG-17	1.43	1500
HTV-1	42	A11	NBG-17	1.49	1500
HTV-1	38	A10	NBG-17	1.56	1500
HTV-1	34	A9	NBG-17	1.58	1500
HTV-2	54	A30	NBG-17	3.5	1500
HTV-2	50	A29	NBG-17	3.85	1500
HTV-2	46	A28	NBG-17	4.28	1500
HTV-2	42	A27	NBG-17	4.48	1500
HTV-2	38	A26	NBG-17	4.69	1500
HTV-2	34	A25	NBG-17	4.75	1500

Table 5.8. Neutron dose per sample in each capsule and temperature zone for grade NBG-18

Capsule	Position	Specimen Number	Grade	Dose, dpa	Temperature, C
HTV-1	8-63	B16	NBG-18	0.75	900
HTV-1	8-59	B15	NBG-18	0.92	900
HTV-1	2-10	B3	NBG-18	1.13	900
HTV-1	2-14	B4	NBG-18	1.26	900
HTV-1	4-28	B7	NBG-18	1.57	900
HTV-1	4-32	B8	NBG-18	1.59	900

Table 5.8. Neutron dose per sample in each capsule and temperature zone for grade NBG-18

Capsule	Position	Specimen Number	Grade	Dose, dpa	Temperature, C
HTV-2	1-3	B17	NBG-18	2.35	900
HTV-2	1-7	B18	NBG-18	2.87	900
HTV-2	3-17	B21	NBG-18	4.16	900
HTV-2	3-21	B22	NBG-18	4.40	900
HTV-2	4-28	B23	NBG-18	4.70	900
HTV-2	4-32	B24	NBG-18	4.76	900
HTV-1	7-54	B14	NBG-18	1.16	1200
HTV-1	7-50	B13	NBG-18	1.29	1200
HTV-1	3-17	B5	NBG-18	1.39	1200
HTV-1	3-21	B6	NBG-18	1.47	1200
HTV-2	8-63	B32	NBG-18	2.24	1200
HTV-2	8-59	B31	NBG-18	2.77	1200
HTV-2	2-10	B19	NBG-18	3.40	1200
HTV-2	2-14	B20	NBG-18	3.79	1200
HTV-2	5-40	B26	NBG-18	4.64	1200
HTV-2	5-36	B25	NBG-18	4.73	1200
HTV-1	1-3	B1	NBG-18	0.78	1500
HTV-1	1-7	B2	NBG-18	0.96	1500
HTV-1	6-45	B12	NBG-18	1.44	1500
HTV-1	6-41	B11	NBG-18	1.51	1500
HTV-1	5-40	B10	NBG-18	1.55	1500
HTV-1	5-36	B9	NBG-18	1.58	1500
HTV-2	7-54	B30	NBG-18	3.49	1500
HTV-2	7-50	B29	NBG-18	3.86	1500
HTV-2	6-45	B28	NBG-18	4.31	1500
HTV-2	6-41	B27	NBG-18	4.52	1500

Table 5.9. Neutron dose per sample in each capsule and temperature zone for grade IG-430

Capsule	Position	Specimen Number	Grade	Dose, dpa	Temperature, C
HTV-1	8-64	F14	IG-430	0.71	900
HTV-1	8-60	F13	IG-430	0.89	900
HTV-1	2-11	F3	IG-430	1.16	900
HTV-1	4-25	F6	IG-430	1.55	900
HTV-2	1-4	F15	IG-430	2.46	900
HTV-2	3-18	F18	IG-430	4-21	900

Table 5.9. Neutron dose per sample in each capsule and temperature zone for grade IG-430

HTV-2	4-25	F19	IG-430	4.64	900
HTV-1	7-55	F12	IG-430	1.13	1200
HTV-1	7-51	F11	IG-430	1.26	1200
HTV-1	3-18	F4	IG-430	1.40	1200
HTV-1	3-22	F5	IG-430	1.48	1200
HTV-2	8-64	F27	IG-430	2.12	1200
HTV-2	8-60	F26	IG-430	2.67	1200
HTV-2	2-11	F16	IG-430	3.49	1200
HTV-2	2-15	F17	IG-430	3.86	1200
HTV-2	5-37	F21	IG-430	4.70	1200
HTV-2	5-33	F20	IG-430	4.76	1200
HTV-1	1-4	F1	IG-430	0.82	1500
HTV-1	1-8	F2	IG-430	0.99	1500
HTV-1	6-46	F10	IG-430	1.42	1500
HTV-1	6-42	F9	IG-430	1.49	1500
HTV-1	5-37	F8	IG-430	1.57	1500
HTV-1	5-33	F7	IG-430	1.59	1500
HTV-2	7-55	F25	IG-430	3.40	1500
HTV-2	7-51	F24	IG-430	3.79	1500
HTV-2	6-46	F23	IG-430	4.26	1500
HTV-2	6-42	F22	IG-430	4.48	1500

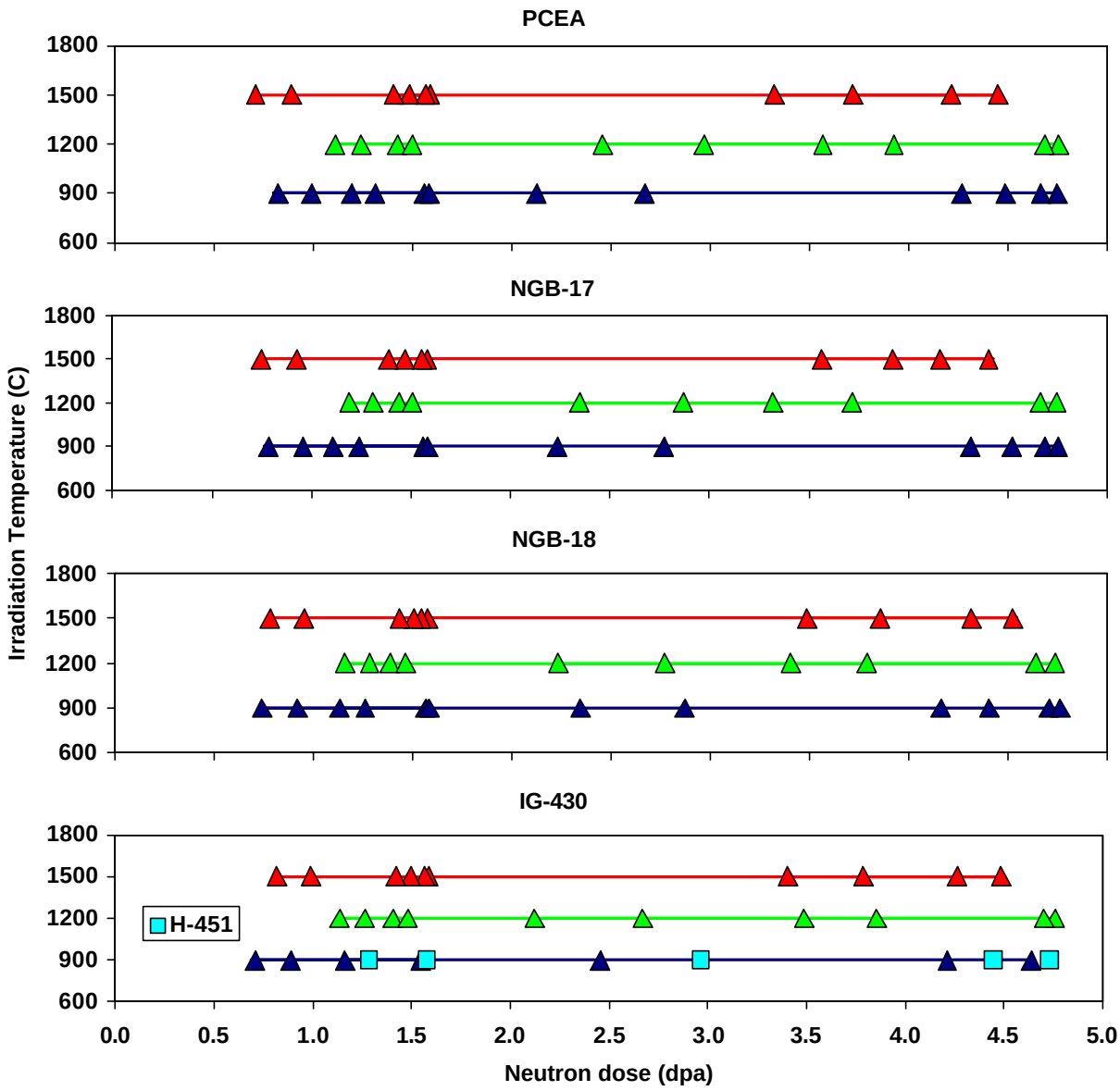

Figure 5.15. Estimated dose (dpa) and temperature distributions for capsules HTV-1 and -2

6. Materials Pre-characterization

Graphite preirradiation examination and characterization will be performed at the Oak Ridge National Laboratory (ORNL) to take advantage of existing facilities and expertise. The graphite billets purchased (or in many cases provided gratis by the vendors) [11] for the HTV capsules will be sectioned and specimens machined in accordance with cutting plans that take into account textural variations within the graphite billets. The cutting plans will be reported in the preirradiation examination report. All graphite samples will be laser engraved with a unique number identifying the graphite grade, location within the billet, and orientation with respect to the forming direction. For the HTV capsules, all graphite specimens will be cut with their length direction parallel to the forming direction.

The following codes will be used to designate the graphite grades included in the HTV capsules.

Table 6.1. Graphite grade marking codes to be used for the HTV series of experiments

Graphite Code Letter	Graphite Grade
A	NBG-17
B	NBG-18
C	H-451
D	PCEA
F	IG-430

All machined specimens shall be subjected to a full dimensional inspection as well as a visual inspection to check for damage and confirm the clarity of the laser marking. Those specimens to be encapsulated in HTV-1 and -2 will be set aside and only non-destructive testing shall be performed on them. The remaining specimens (controls) shall be tested to determine key physical properties as detailed below. Where possible, the testing will be carried out in accordance with the appropriate American Society for Testing and Materials (ASTM) specification(s) [12]. Figure 6.1 shows the preirradiation test program schematically. Non-destructive measurements to be performed include: dimensions; mass (hence bulk density); elastic modulus by the sonic velocity method, yielding Young's modulus, Shear modulus, and Poisson's ratio; thermal flash diffusivity at room temperature and as a function of temperature (25-1200°C), and hence the thermal conductivity. These measurements will be made on all of the specimens to be encapsulated in HTV-1 and -2, with the exception of the elevated temperature thermal diffusivity which will be performed on a statistically representative sample of the control (unirradiated) specimens. Additional destructive tests to be performed on the companion samples include: X-ray diffraction (XRD) on powdered samples of the graphites (and hence the crystallographic parameters a, c, l_a, l_c); microstructural characterization via optical microscopy, scanning electron microscopy, and Hg-porosymmetry (hence grain-size and pore-size distributions); finally, strength tests of the specimens, the test type being dependant upon the specimen geometry, will provide compressive strength data.

The determination of which tests are applied to which specimens is influenced by a number of considerations, including sample geometry, graphite texture, statistical factors, test equipment availability, test duration and complexity, and cost/budget. The data that are produced will support not only the NGNP irradiation effects program, but will provide valuable data for ongoing efforts in code and model development; e.g., the ASME design code for graphite core components. Analysis of the preirradiation data must take into account factors such as statistical variations, textural effects, and volume effects (irradiation specimens are, of necessity, very small volume).

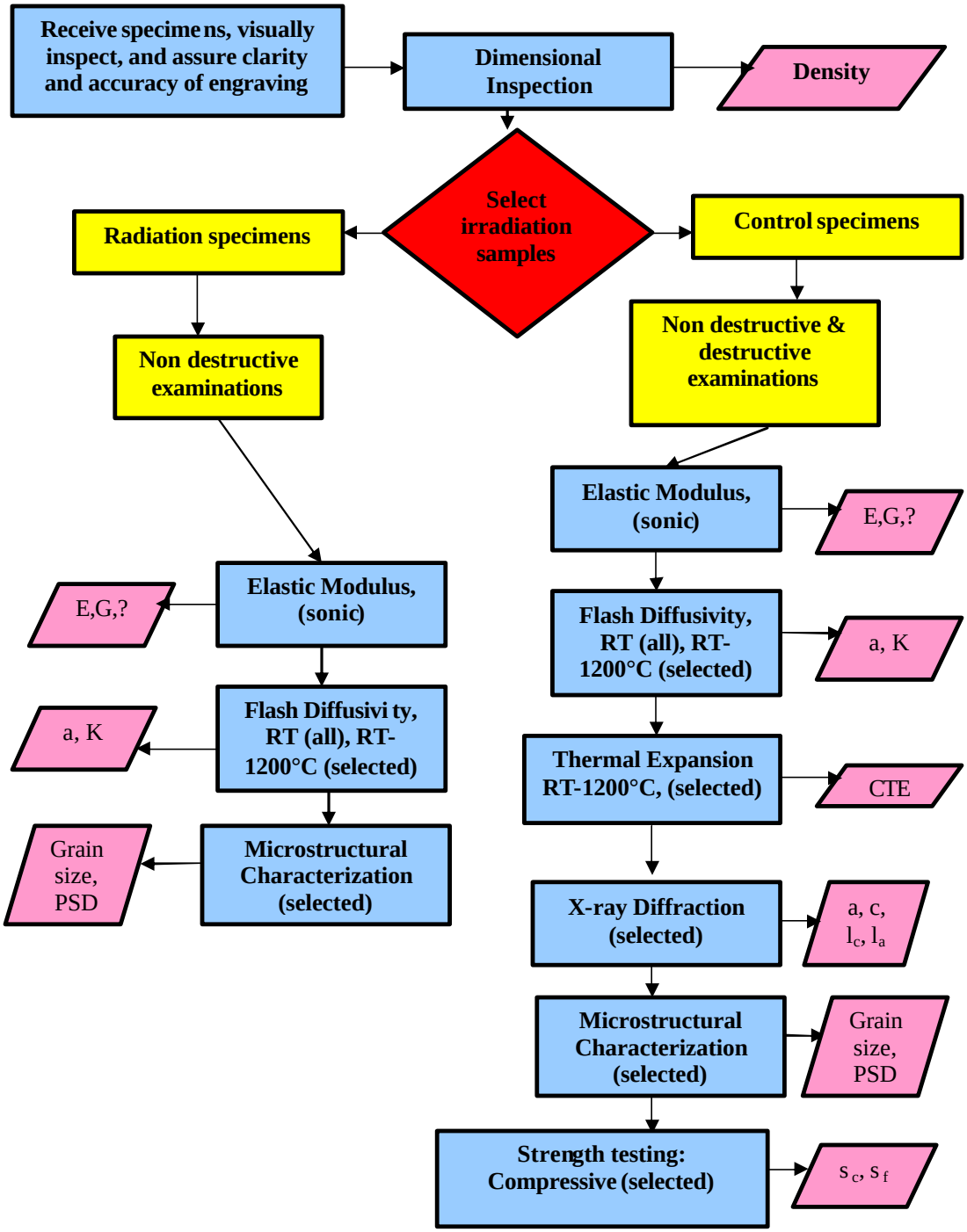

Figure 6.1. Preirradiation data process flow chart for irradiation experiments HTV-1 and -2

The preirradiation characterization and testing of graphites for the HTV experiments will be reported in a preirradiation data report and in electronic format (spreadsheets). The preirradiation report will include details of the following:

- Graphite grades and billet sizes
- Cutting plans
- Specimen numbering scheme
- Test/experimental methods
- Revised HTV-1 and -2 layouts (loading plans) with specimens identity numbers
- Tabulated data by grade
- Specific preirradiation data on the HTV-1 and -2 encapsulated specimens
- Preirradiation data from HTV-1 and -2 control specimens
- Analysis and discussion of the preirradiation data

7. Post-irradiation Examination

Following completion of the specified irradiation period, the HTV-1 and -2 capsules contents will be subjected to postirradiation examination (PIE). The anticipated PIE process is illustrated in Figure 7.1.

After the requisite time in the cooling ponds at HFIR, the capsule will be shipped in a commercial cask to the NNFD Hot Cells at ORNL for disassembly. The flux wires will be removed for testing (gamma scans) and the data used to calibrate the dose model. The graphite specimens and SiC temperature monitors will be visually inspected and packaged for shipment to the Bldg. 4508 hot labs where PIE will be conducted. Prudent engineering practice dictates that the PIE should be conducted at the same laboratory as the preirradiation examination. This precludes the occurrence of bias in the data which can originate from differences in test methods and machines, instruments, and personnel. PIE of the melt-materials will provide additional data to calibrate the thermal model and allow accurate determinations of the irradiation temperature.

All of the samples will be subjected to full dimensional analysis and will be weighed for bulk density determinations. The exact nature and order of the PIE measurements depends upon irradiation sample geometry, the destructive tests being performed last. Critical PIE data for the HTV-1 and -2 experiments are those data related to the irradiation-induced dimensional change behavior and its analysis (as described in Sections 2 & 3). HTV-1 and -2 graphite PIE data will support model development in the areas of irradiation induced-dimensional change behavior, thermal conductivity, and fracture behavior. Additional PIE data to be obtained from the graphite specimens include:

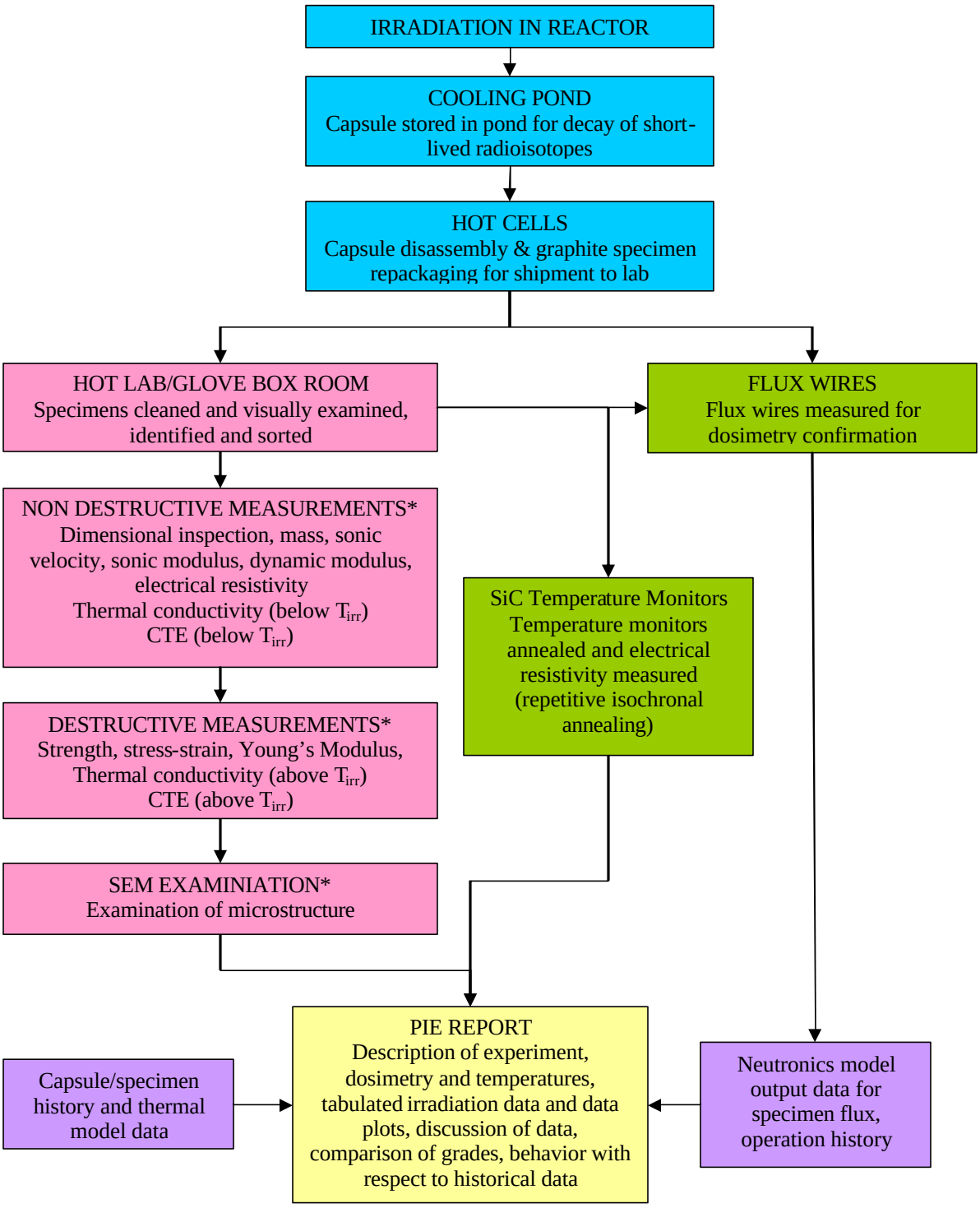

Figure 7.1. The postirradiation examination process for HFIR experiments HTV-1 and-2

- Elastic constants (Young's modulus, E; Shear modulus, G; Poisson's ratio, ?)
- Thermal conductivity, room temperature, and elevated temperature
- Compressive strength
- Microstructural characterization

The PIE data shall be reported in a PIE report(s) that will give details of the measurements made, the experimental flux and thermal data, the revised dosimetry and temperature estimates, graphite PIE data, and analysis [11].

8. Schedule

The planned schedule for Capsules HTV-1 and -2 is shown in Table 8.1.

Table 8.1. Planned schedule for Capsules HTV-1 and -2

TASK	Due Date
Issue draft experimental plan and preliminary design report	9-30-05
Issue draft final capsule design report	8-31-06
Initiate capsule construction	8-31-06
Complete preirradiation examination of HTV-1 and -2 graphite specimens	9-30-06
Complete assembly of HTV-1	3-31-07
Complete assembly of HTV-2	3-31-07
Insert HTV-1 and -2 in HFIR	6-30-07
Complete irradiation of HTV-1	8-31-07
Complete hot cell disassembly of HTV-1	10-31-07
Complete irradiation of HTV-2	12-31-07
Complete hot cell disassembly of HTV-2	2-28-08
Complete graphite PIE	6-30-08
Issue draft HTV-1 and -2 PIE report	9-30-08

9. Acknowledgements

This work is sponsored by the U.S. Department of Energy, Office of Nuclear Energy Science and Technology under contract DE-AC05-00OR22725 with Oak Ridge National Laboratory, managed by UT-Battelle, LLC.

10. References

1. Burchell, T. and Bratton, R., *Graphite Irradiation Creep Capsule AGC-1 Experimental Plan*, ORNL/TM-2005/505 (May 2005)

2. Simmons, J.W.H., *Radiation Damage in Graphite*. 1965: Pergamon, New York, London

3. Nightingale, R.E., *Nuclear Graphite*. 1962: Academic Press

4. Kennedy, C.R. and E.M. Woodruff, *Irradiation Effects on the Physical Properties of Grade TSX Graphite*. 1989, Westinghouse Hanford Company: Richland Washington

5. Burchell, T.D. and A.J. Wickham. *The Dimensional Change in Pile Grade A Graphite Irradiated in CEGB Magnox Power Reactors*. in *Proc. CARBON '87, 18th Biennial Conf on Carbon*. 1987

6. Burchell, T.D. *Neutron Irradiation Damage in Graphite and its Effects on Properties*, CARBON '02, 15-19 September 2002. Beijing, China

7. The Industrial Graphite Engineering Handbook, Pub. UCAR Carbon Company, Inc., (1991) p. 5B.07

8. MCNP — A General Monte Carlo N-Particle Transport Code, Version 5, 2003.

9. ANSYS, Inc., Finite Element Software, Release 10.0, 2005.

10. I. C. Gauld, O. W. Herman, and R. M. Westfall, *ORIGEN-S: SCALE System Module to Calculate Fuel Depletion, Actinide Transmutation, Fission Product Buildup and Decay, and Associated Radiation Source Terms*, Vol. II, Sect. F7, ORNL/NUREG/CSD-2/V2/R7.

11. R. Bratton and T. Burchell, Milestone Report: NGNP Graphite Selection Strategy, INL/EXT-05-00269, (2005)

12. ASTM C-781 "*Standard Practice for Testing Graphite and Boronated Components for High-Temperature Gas-Cooled Nuclear Reactors*" ASTM Standards Vol. 05.05, ASTM International, West Conshohocken, PA, (2005)

11. ASTM C-625 "*Standard Practice for Reporting Irradiation Results on Graphite*" ASTM Standards Vol. 05.05, ASTM International, West Conshohocken, PA, (2005)

Appendix 1. Specimen Layout in Capsules HTV-1 and HTV-2

Sub-capsule	Pos.	Distance from HMP		Est. flux ratio	Graphite grade	HTV-1					HTV-2				
						Design Temp., °C	Spec. No.	Specimen OD		Est. Fluence, dpa	Design Temp., °C	Spec. No.	Specimen OD		Est. Fluence, dpa
		in.	cm					in.	mm				in.	mm	
1	1-1	9.59	24.36	0.445	PCEA	1500	D1	0.300	7.62	0.71	900	D17	0.400	10.16	2.12
	1-2	9.38	23.83	0.469	NBG-17	1500	A1	0.300	7.62	0.75	900	A17	0.400	10.16	2.24
	1-3	9.17	23.29	0.493	NBG-18	1500	B1	0.300	7.62	0.78	900	B17	0.400	10.16	2.35
	1-4	8.96	22.76	0.516	IG-430	1500	F1	0.300	7.62	0.82	900	F15	0.400	10.16	2.46
	1-5	8.54	21.69	0.560	PCEA	1500	D2	0.300	7.62	0.89	900	D18	0.400	10.16	2.67
	1-6	8.33	21.16	0.581	NBG-17	1500	A2	0.300	7.62	0.92	900	A18	0.400	10.16	2.77
	1-7	8.12	20.62	0.602	NBG-18	1500	B2	0.300	7.62	0.96	900	B18	0.400	10.16	2.87
	1-8	7.91	20.09	0.623	IG-430/H-451	1500	F2	0.300	7.62	0.99	900	C3	0.400	10.16	2.97
2	2-9	7.09	18.01	0.697	NBG-17	900	A3	0.400	10.16	1.11	1200	A19	0.400	10.16	3.32
	2-10	6.88	17.48	0.714	NBG-18	900	B3	0.400	10.16	1.13	1200	B19	0.400	10.16	3.40
	2-11	6.67	16.94	0.732	IG-430	900	F3	0.400	10.16	1.16	1200	F16	0.400	10.16	3.49
	2-12	6.46	16.41	0.748	PCEA	900	D3	0.400	10.16	1.19	1200	D19	0.400	10.16	3.56
	2-13	6.04	15.34	0.780	NBG-17	900	A4	0.400	10.16	1.24	1200	A20	0.400	10.16	3.72
	2-14	5.83	14.81	0.795	NBG-18	900	B4	0.400	10.16	1.26	1200	B20	0.400	10.16	3.79
	2-15	5.62	14.27	0.809	H-451/IG-430	900	C1	0.400	10.16	1.29	1200	F17	0.400	10.16	3.86
	2-16	5.41	13.74	0.823	PCEA	900	D4	0.400	10.16	1.31	1200	D20	0.400	10.16	3.92
3	3-17	4.59	11.66	0.873	NBG-18	1200	B5	0.400	10.16	1.39	900	B21	0.400	10.16	4.16
	3-18	4.38	11.13	0.884	IG-430	1200	F4	0.400	10.16	1.40	900	F18	0.400	10.16	4.21
	3-19	4.17	10.59	0.895	PCEA	1200	D5	0.400	10.16	1.42	900	D21	0.400	10.16	4.26
	3-20	3.96	10.06	0.905	NBG-17	1200	A5	0.400	10.16	1.44	900	A21	0.400	10.16	4.31
	3-21	3.54	8.99	0.924	NBG-18	1200	B6	0.400	10.16	1.47	900	B22	0.400	10.16	4.40
	3-22	3.33	8.46	0.933	IG-430/H-451	1200	F5	0.400	10.16	1.48	900	C4	0.400	10.16	4.45
	3-23	3.12	7.92	0.941	PCEA	1200	D6	0.400	10.16	1.49	900	D22	0.400	10.16	4.48
	3-24	2.91	7.39	0.949	NBG-17	1200	A6	0.400	10.16	1.51	900	A22	0.400	10.16	4.52
4	4-25	2.09	5.31	0.974	IG-430	900	F6	0.400	10.16	1.55	900	F19	0.400	10.16	4.64
	4-26	1.88	4.78	0.979	PCEA	900	D7	0.400	10.16	1.55	900	D23	0.400	10.16	4.66
	4-27	1.67	4.24	0.983	NBG-17	900	A7	0.400	10.16	1.56	900	A23	0.400	10.16	4.68
	4-28	1.46	3.71	0.987	NBG-18	900	B7	0.400	10.16	1.57	900	B23	0.400	10.16	4.70
	4-29	1.04	2.64	0.993	H-451	900	C2	0.400	10.16	1.58	900	C5	0.400	10.16	4.73
	4-30	0.83	2.11	0.996	PCEA	900	D8	0.400	10.16	1.58	900	D24	0.400	10.16	4.74
	4-31	0.62	1.57	0.998	NBG-17	900	A8	0.400	10.16	1.58	900	A24	0.400	10.16	4.75
	4-32	0.41	1.04	0.999	NBG-18	900	B8	0.400	10.16	1.59	900	B24	0.400	10.16	4.76

Appendix 1. Specimen Layout in Capsules HTV-1 and HTV-2

Sub-capsule	Pos.	Distance from HMP		Est. flux ratio	Graphite grade	HTV-1					HTV-2				
						Design Temp., °C	Spec. No.	Specimen OD		Est. Fluence, dpa	Design, Temp., °C	Spec. No.	Specimen OD		Est. Fluence, dpa
		in.	cm					in.	mm				in.	mm	
5	5-33	-0.41	-1.04	0.999	IG-430	1500	F7	0.400	10.16	1.59	1200	F20	0.400	10.16	4.76
	5-34	-0.62	-1.57	0.998	PCEA	1500	D9	0.400	10.16	1.58	1200	D25	0.400	10.16	4.75
	5-35	-0.83	-2.11	0.996	NBG-17	1500	A9	0.400	10.16	1.58	1200	A25	0.400	10.16	4.74
	5-36	-1.04	-2.64	0.993	NBG-18	1500	B9	0.400	10.16	1.58	1200	B25	0.400	10.16	4.73
	5-37	-1.46	-3.71	0.987	IG-430	1500	F8	0.400	10.16	1.57	1200	F21	0.400	10.16	4.70
	5-38	-1.67	-4.24	0.983	PCEA	1500	D10	0.400	10.16	1.56	1200	D26	0.400	10.16	4.68
	5-39	-1.88	-4.78	0.979	NBG-17	1500	A10	0.400	10.16	1.55	1200	A26	0.400	10.16	4.66
	5-40	-2.09	-5.31	0.974	NBG-18	1500	B10	0.400	10.16	1.55	1200	B26	0.400	10.16	4.64
6	6-41	-2.91	-7.39	0.949	NBG-18	1500	B11	0.350	8.89	1.51	1500	B27	0.350	8.89	4.52
	6-42	-3.12	-7.92	0.941	IG-430	1500	F9	0.350	8.89	1.49	1500	F22	0.350	8.89	4.48
	6-43	-3.33	-8.46	0.933	PCEA	1500	D11	0.350	8.89	1.48	1500	D27	0.350	8.89	4.45
	6-44	-3.54	-8.99	0.924	NBG-17	1500	A11	0.350	8.89	1.47	1500	A27	0.350	8.89	4.40
	6-45	-3.96	-10.06	0.905	NBG-18	1500	B12	0.350	8.89	1.44	1500	B28	0.350	8.89	4.31
	6-46	-4.17	-10.59	0.895	IG-430	1500	F10	0.350	8.89	1.42	1500	F23	0.350	8.89	4.26
	6-47	-4.38	-11.13	0.884	PCEA	1500	D12	0.350	8.89	1.40	1500	D28	0.350	8.89	4.21
	6-48	-4.59	-11.66	0.873	NBG-17	1500	A12	0.350	8.89	1.39	1500	A28	0.350	8.89	4.16
7	7-49	-5.41	-13.74	0.823	NBG-17	1200	A13	0.400	10.16	1.31	1500	A29	0.350	8.89	3.92
	7-50	-5.62	-14.27	0.809	NBG-18	1200	B13	0.400	10.16	1.29	1500	B29	0.350	8.89	3.86
	7-51	-5.83	-14.81	0.795	IG-430	1200	F11	0.400	10.16	1.26	1500	F24	0.350	8.89	3.79
	7-52	-6.04	-15.34	0.780	PCEA	1200	D13	0.400	10.16	1.24	1500	D29	0.350	8.89	3.72
	7-53	-6.46	-16.41	0.748	NBG-17	1200	A14	0.400	10.16	1.19	1500	A30	0.350	8.89	3.56
	7-54	-6.67	-16.94	0.732	NBG-18	1200	B14	0.400	10.16	1.16	1500	B30	0.350	8.89	3.49
	7-55	-6.88	-17.48	0.714	IG-430	1200	F12	0.400	10.16	1.13	1500	F25	0.350	8.89	3.40
	7-56	-7.09	-18.01	0.697	PCEA	1200	D14	0.400	10.16	1.11	1500	D30	0.350	8.89	3.32
8	8-57	-7.91	-20.09	0.623	PCEA	900	D15	0.400	10.16	0.99	1200	D31	0.350	8.89	2.97
	8-58	-8.12	-20.62	0.602	NBG-17	900	A15	0.400	10.16	0.96	1200	A31	0.350	8.89	2.87
	8-59	-8.33	-21.16	0.581	NBG-18	900	B15	0.400	10.16	0.92	1200	B31	0.350	8.89	2.77
	8-60	-8.54	-21.69	0.560	IG-430	900	F13	0.400	10.16	0.89	1200	F26	0.350	8.89	2.67
	8-61	-8.96	-22.76	0.516	PCEA	900	D16	0.400	10.16	0.82	1200	D32	0.350	8.89	2.46
	8-62	-9.17	-23.29	0.493	NBG-17	900	A16	0.400	10.16	0.78	1200	A32	0.350	8.89	2.35
	8-63	-9.38	-23.83	0.469	NBG-18	900	B16	0.400	10.16	0.75	1200	B32	0.350	8.89	2.24
	8-64	-9.59	-24.36	0.445	IG-430	900	F14	0.400	10.16	0.71	1200	F27	0.350	8.89	2.12

Distribution

1. T. D. Burchell
2. W. R. Corwin
3. S. R. Greene
4. D. Heatherly
5. D. T. Ingersoll
6. Y. Katoh
7. J. W. Klett
8. E. Lara-Curzio
9. T. E. McGreevy
10. L. K. Mansur
11 J. McDuffee
12. R. K. Nanstad
13. R. A. Raschke
14. W. Ren
15. P. L. Rittenhouse
16. A. F. Rowcliff
17. L. L. Snead
18. R. G. Stoller
19. R. W. Swindeman
20. K. Thoms
21. P. F. Tortorelli
22. D. F. Wilson
23. G. L. Yoder, Jr.
24. S. J. Zinkle

25. Cathy Barnard, Idaho National Engineering and Environmental Laboratory, P.O. Box 1625, Idaho Falls, Idaho 83415-3750

26. Robert Bratton, Idaho National Engineering and Environmental Laboratory, P.O. Box 1625, Idaho Falls, Idaho 83415-3710

27. Trevor Cook, NE-20/Germantown Building, Office of Advanced Nuclear Research, U.S. Department of Energy, 1000 Independence Avenue, S.W., Washington, DC 20585-1290

28. Susan Lesica, NE-20/Germantown Building, Office of Advanced Nuclear Research, U.S. Department of Energy, 1000 Independence Avenue, S.W., Washington, DC 20585-1290

29. Thomas J. O'Conner, NE-20/Germantown Building, Office of Advanced Nuclear Research, U.S. Department of Energy, 1000 Independence Avenue, S.W., Washington, DC 20585-1290

30. Robert Versluis, NE-20/Germantown Building, Office of Advanced Nuclear Research, U.S. Department of Energy, 1000 Independence Avenue, S.W., Washington, DC 20585-1290

31. Kevan Weaver, Idaho National Engineering and Environmental Laboratory, P.O. Box 1625, Idaho Falls, Idaho 83415-3750